Chapter-1

Introduction and Literature Review

CHAPTER 1

Introduction and Literature Review

1.1 Motivation and General Introduction

The quest for sustainable and environmentally friendly energy solutions has spurred significant interest in piezoelectric materials, especially for energy harvesting technologies. These materials can convert mechanical stress into electrical energy, making them ideal for powering electronic devices in remote or inaccessible environments. Historically, lead zirconate titanate, $PbZr_xTi_{1-x}O_3$ (PZT) has dominated the field due to its exceptional electromechanical properties [1]. Since its introduction in the 1950s, PZT has been the dominant piezoelectric material. Its properties have been continually enhanced through improvements in chemistry, microstructure, and processing techniques [2]. In 2022, the piezoelectric materials market was valued at USD 1.5 billion, with projections reaching USD 2.287 billion by 2032 as mentioned in Figure 1.1, driven by factors like aerospace applications, automotive industry demand, and automation [3]. However, the environmental and health hazards posed by lead based compounds have driven research towards lead-free alternatives. Stringent environmental regulations, technological advancements, and the increasing demand for sustainable technologies are the primary growth drivers. The lead-free piezoelectric materials market is projected to grow at a compound annual growth rate (CAGR) of approximately 8-10% from 2021 to 2028, with a market value expected to reach between USD 2.5 billion and USD 3 billion by 2028 [3]. This growth is fueled by the demand for miniaturized electronic devices, the shift towards electric vehicles in the automotive industry, advancements in aerospace and defense applications, and the healthcare sector's need for safe and compliant medical devices.

Despite challenges such as achieving performance parity with lead-based materials and higher production costs, ongoing research and development efforts are enhancing the properties and competitiveness of lead-free alternatives. Supportive regulations and emerging applications in energy harvesting technologies present significant growth opportunities for lead-free piezoelectric materials in the coming years.

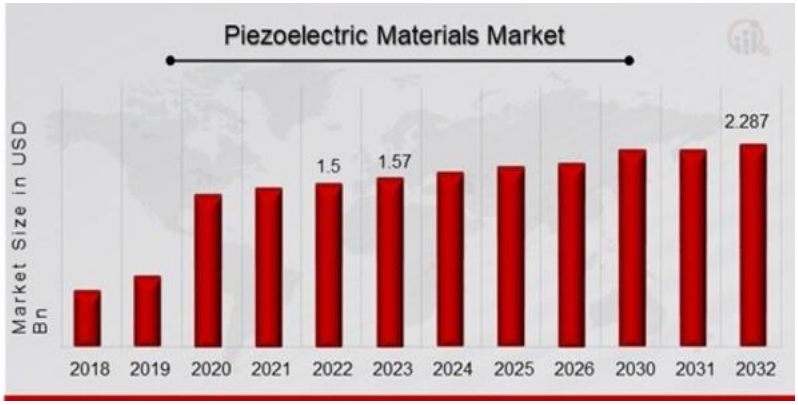

Figure 1.1 Piezoelectric materials market share by 2032 (in USD Billion) (adopted from [3]).

The demand for advanced piezoelectric materials spans a wide range of applications in sensors, actuators, transducers and energy harvesting devices, ranging from aerospace to telecommunications. Numerous discoveries in recent years have revealed that a single compound is unlikely to replace lead-containing materials across the entire spectrum of applications. As industries push towards sustainable development and high-performance materials, the focus has shifted towards developing piezoelectrics that not only perform under extreme conditions but are also environmentally benign.

Within the category of lead-free bulk piezoelectric systems, compounds such as $K_{0.5}Na_{0.5}NbO_3$ (KNN), $BaTiO_3$ (BT), $Bi_{0.5}Na_{0.5}TiO_3$ (BNT), $BiFeO_3$ (BFO), $Bi_4Ti_3O_{12}$ (BIT) and their binary and ternary modified solid solutions have emerged as promising candidates, exhibiting properties comparable to those of lead-based systems [4]. High

temperature piezoelectrics are crucial in sectors such as aerospace, deep-sea exploration, and energy generation, where materials must endure temperatures of approximately 300 °C or higher [5]. High-temperature piezoelectric energy harvesting presents an intriguing and challenging area of exploration, characterized by factors such as temperature stability, phase behavior, and efficient conversion of heat and mechanical energy into electrical energy, while considering reproducibility and loss mechanisms. Among the various candidates for lead-free piezoelectric materials, Bi-based perovskite ceramics have shown considerable potential. These materials not only comply with global environmental directives such as the Restriction of Hazardous Substances (RoHS) Directive but also exhibit promising piezoelectric and ferroelectric properties [6], [7], [8], [9], [10]**.** These materials promise to combine high-temperature resilience with robust piezoelectric properties, making them ideal for applications where traditional piezoelectrics falter. The potential to harness energy from environmental and industrial waste—such as mechanical stress and excess heat in automotive or aerospace settings—positions Bi-based ceramics as key enablers of energy-efficient and sustainable technologies. The $BiFeO_3$-$BaTiO_3$ (BF-BT) solid solution and $Bi_4Ti_3O_{12}$ demonstrate particularly promising properties for high-temperature applications, owing to a high Curie temperature and excellent dielectric, piezoelectric, magnetic, and ferroelectric properties [11], [12].

The motivation for this thesis is rooted in developing a deeper understanding of Bi-based lead-free piezoelectric ceramics, focusing on their structural and functional viability for high-temperature energy harvesting applications. By exploring novel compositions and fabrication techniques, this research aims to unveil materials that not only meet the technical demands of modern industry but also align with global environmental and health standards. The ultimate goal is to contribute to the field of

electroceramics by introducing innovative materials that could redefine the benchmarks for performance and sustainability in piezoelectric technology.

Before delving into our investigation of various compositions of Bi-based high-temperature ceramics, we will provide an overview of the essential terms and concepts necessary for understanding the subject. Following this, we will present a concise review of the existing literature and the current state of research on this topic. The chapter will conclude with a statement of the main objectives of this thesis.

1.2 Fundamentals of Dielectrics

1.2.1 Introduction to Dielectrics

Dielectrics are materials that are poor conductors of electricity but efficient supporters of electrostatic fields. They can be polarized by an applied electric field, which means they exhibit dipole moments that align with the field. The ability to support electrostatic fields while dissipating minimal energy makes them crucial in various applications like capacitors, insulators, and more.

1.2.1.1 Mathematical Description of Polarization

The macroscopic polarization (P) in a dielectric material can be expressed as the sum of all individual dipole moments per unit volume. The relationship between P and the electric field (E) is given by:

$$\boldsymbol{P} = \boldsymbol{\varepsilon_0} * \boldsymbol{\chi} * \boldsymbol{E} \qquad (1.1)$$

where $\boldsymbol{\varepsilon_0}$ is the permittivity of free space (= 8.854 * 10^{-12} F/m) and $\boldsymbol{\chi}$ is the electric susceptibility of the material.

The physical quantity corresponding to the stored electric charge per unit area is called the electric displacement *D*, which relates to the *E* and P as follows:

$$\boldsymbol{D} = \boldsymbol{\varepsilon_0 E} + \boldsymbol{P} \qquad (1.2)$$

The dielectric susceptibility (χ) can also be expressed using the relative dielectric permittivity or dielectric constant (ε_r):

$$\chi = \varepsilon_r - 1 \quad (1.3)$$

It's important to note that ε_r is not a constant but varies with temperature, frequency, and other factors.

Another important term is polarizability which is defined as the extent to which the dipole moments present in a dielectric material can align with the electric field:

$$p = \alpha E' \quad (1.4)$$

where p is the average dipole moment and E' is the local electric field.

1.2.2 Polarization Mechanisms

Dielectrics can be categorized based on their polarization mechanisms. These mechanisms include electronic polarization, ionic/atomic polarization, orientation/dipolar polarization, and space charge/interfacial polarization as illustrated in Figure 1.2 and 1.3.

Types of Polarization Mechanisms

1. Electronic Polarization: This occurs when the electric field displaces the negatively charged electrons relative to the positively charged nucleus. It is present in all dielectrics and depends on the volume of the electron cloud.
2. Ionic Polarization: In ionic crystals, the electric field causes a relative displacement between positive and negative ions.
3. Orientation Polarization: Found in materials with permanent dipole moments, which align with the electric field. Occurs in materials with permanent dipole moments that align with an electric field. This type of polarization is dependent on the temperature and the strength of the electric field.

4. Space Charge Polarization: Arises due to the accumulation of charges at interfaces or grain boundaries within the material. This can be particularly significant in heterogeneous materials and at high fields. One special case of interfacial polarization is Maxwell-Wagner polarization which occurs at the boundaries between different dielectrics due to their differing conductivities. This leads to charge build-up at the interface and a time-dependent polarization known as Maxwell-Wagner relaxation.

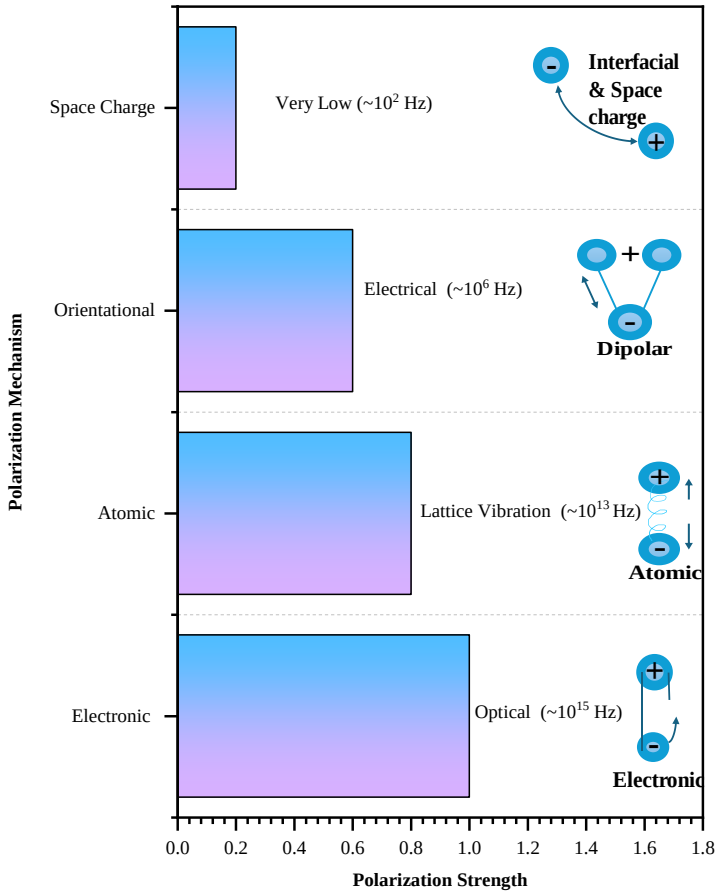

Figure 1.2 Different polarization mechanisms with respect to frequency in dielectrics.

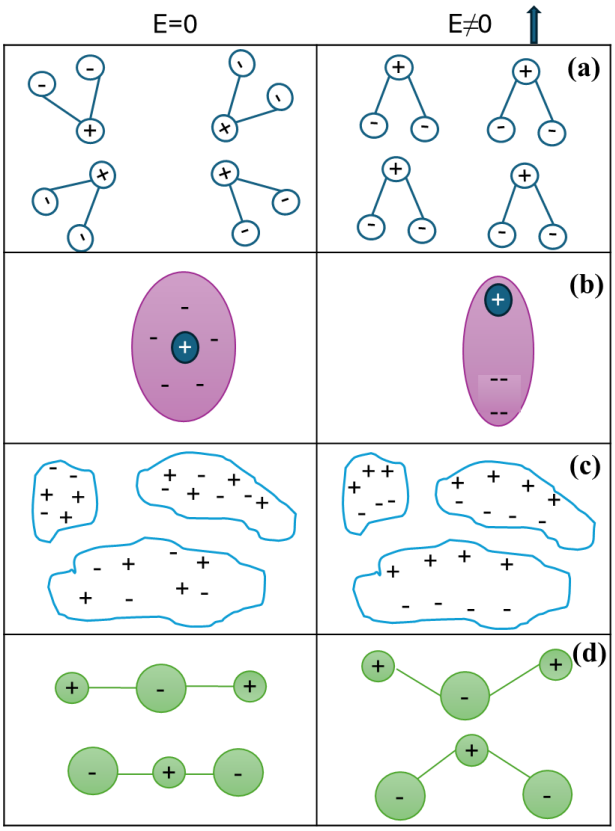

Figure 1.3 Different polarization mechanisms in both presence and absence of applied electric field (a) Dipolar/Orientational/Molecular, (b) Electronic, (c) Interfacial/Space charge and (d) Ionic/ Atomic.

Dielectrics exhibit various polarization mechanisms that contribute to their overall behavior in an electric field. Understanding these mechanisms, their dependencies on material properties and external conditions like temperature and frequency, is crucial for their effective application in technology and industry.

1.3 Basics of Piezoelectricity

Dielectrics can be divided into two types: polar dielectrics, which exhibit spontaneous polarization and thus have a unique polar axis, and non-polar dielectrics, which do not

have this characteristic. As depicted in Figure 1.4 piezoelectrics are subset of dielectrics. Among 32 point groups in accordance with crystallographic symmetry only 21 point groups are non-centrosymmetric which is a necessary condition to exhibit piezoelectricity. With an exception, Point group 432 among these 21 point group doesn't show piezoelectricity. Out of 20 point groups which are piezoelectric 10 are polar and hence pyroelectric which demonstrate polarization as a result of change in temperature (see Table 1.1) [13].

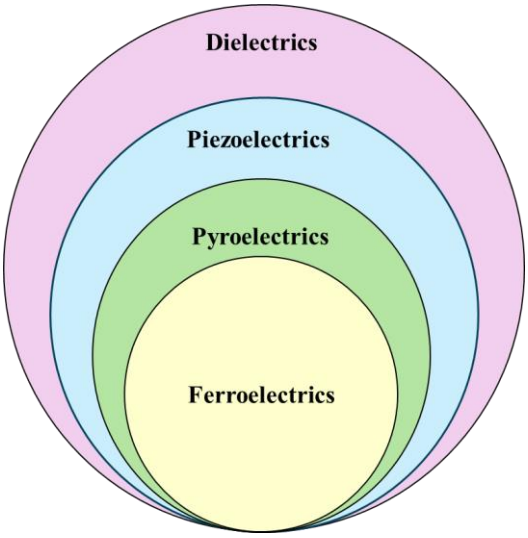

Figure 1.4 Categorization of dielectric materials.

The word "piezo" is derived from the Greek word meaning "pressure," and thus piezoelectricity initially referred to "pressure electricity." In 1880, Pierre and Jacques Curie discovered the direct piezoelectric effect in single crystal quartz. This phenomenon occurs when quartz is placed under pressure, resulting in the generation of an electric charge or voltage. Additionally, materials demonstrating this effect can also exhibit a geometric strain proportional to an applied electric field, which is referred to as the converse piezoelectric effect, discovered by Gabriel Lippmann in 1881.

Table 1.1 Classification of crystallographic point groups using short Hermann-Mauguin Notation based on symmetry.

Crystal Class	**Centrosymmetric**	**Non-centrosymmetric**	
	Non-Polar	*Non-Polar*	*Polar*
Cubic	m$\bar{3}$m, m$\bar{3}$	432, 4$\bar{3}$m, 23	
Hexagonal	6/mmm, 6/m	622, $\bar{6}$m2, $\bar{6}$	6mm, 6
Tetragonal	4/mmm, 4/m	422, $\bar{4}$2m, $\bar{4}$	4mm, 4
Rhombohedral	$\bar{3}$m, $\bar{3}$	32	3m, 3
Orthorhombic	mmm	222	mm2
Monoclinic	2/m		2, m
Triclinic	$\bar{1}$		1
No. of Point Groups	**11**	**11**	**10**

Pierre Curie's recognition of the relationship between these two phenomena allowed him to develop pioneering ideas about the importance of symmetry in the laws of physics. The piezoelectric effect involves the generation of electric charge in certain materials when they are mechanically stressed. There are two types of piezoelectric effects: direct and converse (indirect). The direct piezoelectric effect occurs when a material generates an electric charge in response to mechanical stress. This effect is utilized in sensors and microphones to convert mechanical stimuli into electrical signals. Conversely, the indirect piezoelectric effect occurs when an electric field applied to a piezoelectric material induces a change in shape or deformation. This effect is employed in actuators and speakers to convert electrical signals into mechanical movements.

This property is intrinsic to non-centrosymmetric crystals, where the lack of a center of symmetry allows for the alignment of electric dipoles under stress. It can be defined by following equations [14], [15]:

$$\boldsymbol{D_i = d_{ijk} \cdot \sigma_{jk} + \varepsilon^{\sigma}_{ik} \cdot E_k} \qquad (1.5)$$

$$\boldsymbol{S_{ij} = s^{E}_{ijkl} \cdot \sigma_{kl} + d^{*}_{ijk} \cdot E_{i}} \qquad (1.6)$$

Equation 1.5 describes direct and indirect piezoelectric effect where $\boldsymbol{D_i}$ is the dielectric displacement and is linked to the stress $\boldsymbol{\sigma_{jk}}$ through the piezoelectric $\boldsymbol{d_{ijk}}$. Likewise, there is a second dielectric component contributed by the permittivity $\boldsymbol{\varepsilon^{\sigma}_{ik}}$ in the presence of an electric field $\boldsymbol{E_k}$. The converse piezoelectric effect is explained by Equation 1.6, where the strain $\boldsymbol{S_{ij}}$ is connected to the electric field $\boldsymbol{E_i}$ via the tensor $\boldsymbol{d^{*}_{ijk}}$. Furthermore, the strain also includes an elastic component, which is described by Hooke's law, involving the compliance $\boldsymbol{s^{E}_{ijkl}}$ and the stress $\boldsymbol{\sigma_{kl}}$. The detailed mathematical description can be found elsewhere [14], [15].

1.4 Overview of Ferroelectrics

Ferroelectricity is a property of certain materials that exhibit spontaneous electric polarization, which can be reversed by the application of an external electric field. This phenomenon, first discovered by Joseph Valasek in Rochelle salt in 1920, has since been identified in a variety of materials, including ceramics, polymers, and crystals [16]. This phenomenon necessitates the presence of polarity within the crystal; thus, it is exclusive to pyroelectric crystal classes. However, simply having a dipole is not sufficient to ensure it can be reversed by an electric field. The required field might exceed the breakdown field, or the dipole could result from an asymmetric and irreversible arrangement of atoms. Electric polarization, the separation of positive and negative charges within a material, is the core concept underlying ferroelectricity. In ferroelectric materials, polarization occurs spontaneously and can be reoriented by an external electric field, distinguishing ferroelectrics from ordinary dielectrics. The displacement of ions within the crystal lattice drives ferroelectricity, with temperature-dependent phase transitions occurring at the Curie temperature. Below this temperature, materials exhibit ferroelectric

properties; above it, they behave as paraelectric. Ferroelectric materials have diverse applications due to their unique properties. They are used in non-volatile memory devices, such as Ferroelectric Random Access Memory (FeRAM), leveraging their ability to retain polarization states without power. Additionally, these materials are crucial in sensors, actuators, and capacitors. Recent interest has focused on their potential in energy harvesting applications, where their capacity to convert mechanical energy into electrical energy is particularly advantageous. Previous works have aimed at discovering new materials with enhanced properties and understanding the fundamental physics of ferroelectric behavior. Advances in thin films and nanostructures have enabled the integration of ferroelectric materials into advanced electronic devices. Notably, the exploration of two-dimensional ferroelectric materials holds promise for creating ultra-thin, flexible, and high-performance devices, with significant implications for flexible electronics and wearable technology. Ferroelectricity remains a vibrant area of study, with ongoing research targeting new materials, improved technologies, and expanded applications. The distinctive properties of ferroelectric materials continue to drive innovation across various technological domains, from memory storage to energy harvesting. Understanding the fundamental mechanisms and potential of ferroelectric materials will likely lead to further breakthroughs, cementing their importance in advancing modern technology.

1.5 Overview of Relaxor Ferroelectrics

Relaxor ferroelectrics are a unique class of ferroelectric materials characterized by their diffuse phase transitions and strong frequency-dependent dielectric properties. Unlike conventional ferroelectrics, which exhibit a sharp phase transition at the Curie temperature, relaxor ferroelectrics display a gradual change in dielectric constant over a

broad temperature range. This distinctive behavior is attributed to the presence of nanoscale regions with different polarizations, known as polar nanoregions (PNRs), which contribute to their complex dielectric response. Relaxor ferroelectrics are typically complex perovskite oxides with the general formula ABO_3, where the A and B sites are occupied by different cations. A well-known example is lead magnesium niobate-lead titanate (PMN-PT), which combines lead magnesium niobate $Pb(Mg_{1/3}Nb_{2/3})O_3$ and lead titanate $PbTiO_3$ [17]. The heterogeneity in the cation distribution at the A and B sites leads to the formation of PNRs, which are crucial for the relaxor behavior. The dielectric properties of relaxor ferroelectrics are highly dependent on temperature and frequency. The dielectric constant exhibits a broad peak around the so-called Burns temperature, above which the PNRs start to form. As the temperature decreases, these regions grow and interact, leading to a diffuse phase transition instead of a sharp one. This results in a wide temperature range where the material exhibits high dielectric permittivity.

1.5.1 Difference between Normal Ferroelectrics and Relaxor Ferroelectrics

Ferroelectric materials are broadly categorized into normal ferroelectrics and relaxor ferroelectrics, each exhibiting distinct behavior and properties. Understanding the differences between these two types of ferroelectrics is crucial for their application in various technological fields. The primary differences between normal and relaxor ferroelectrics involve their phase transition behavior, dielectric properties, polarization dynamics, microstructure, and electromechanical responses. Normal ferroelectrics exhibit sharp phase transitions and uniform polarization, making them suitable for stable applications. In contrast, relaxor ferroelectrics display diffuse transitions and complex polarization due to PNRs, making them ideal for applications requiring high dielectric

constants and tunable properties. Figure 1.5 highlights these differences, providing a comparative analysis essential for understanding the unique behaviors.

(a) Polarization-Electric Field (P-E) Hysteresis Loops

- Normal Ferroelectrics: The left panel in Figure 1.5 (a) shows a typical hysteresis loop for normal ferroelectrics, characterized by a sharp and well-defined shape. This indicates the presence of macroscopic ferroelectric (FE) domains that switch direction upon applying an external electric field. The large remnant polarization and coercive field are clearly observable, signifying strong ferroelectric behavior.
- Relaxor Ferroelectrics: In contrast, the right panel in Figure 1.5 (a) for relaxor ferroelectrics depicts a slim hysteresis loop. This indicates the presence of nanoscale polar regions that contribute to the polarization. The coercive field, E_c is still present, but the overall loop shape reflects the more gradual and distributed nature of polarization switching in these materials. Under sufficiently high electric fields, the nanodomains in relaxor ferroelectrics can align with the field, resulting in a significant polarization. However, when the field is removed, most of these domains return to their random orientations, leading to a small remnant polarization, P_r. This small P_r indicates that there is some level of cooperative freezing of the dipolar (or nanodomain) orientations.

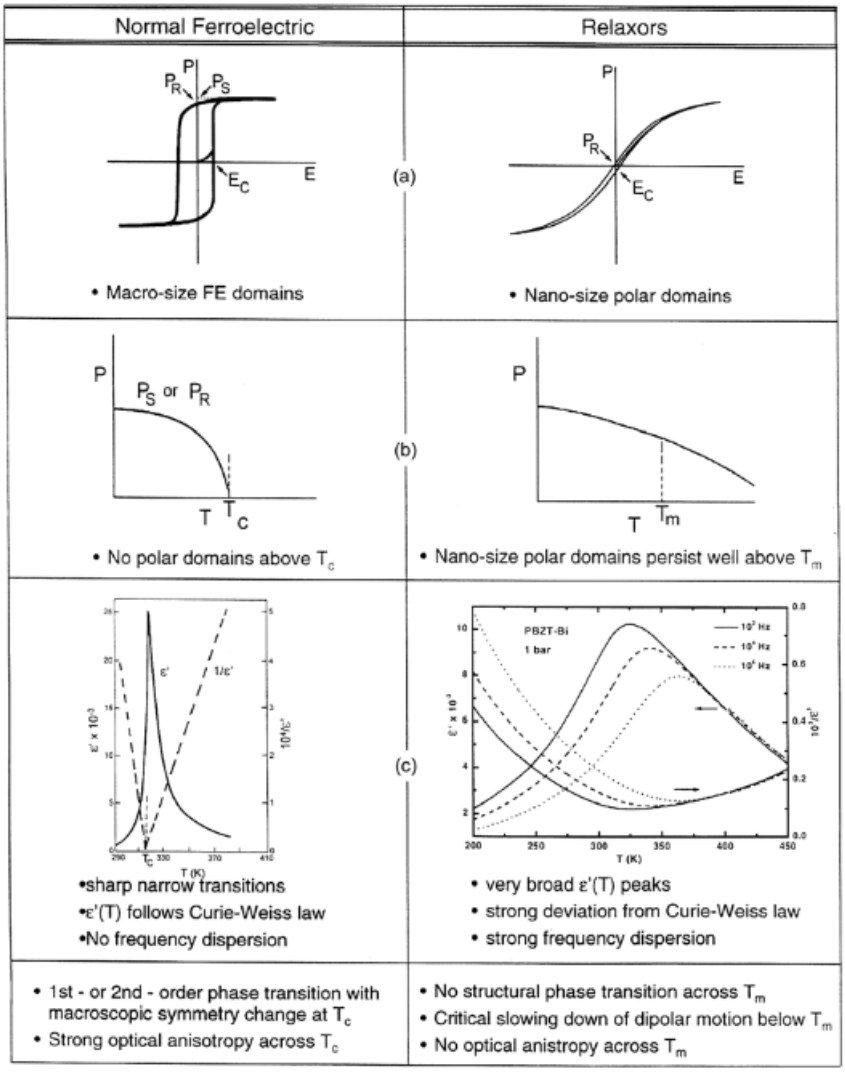

Figure 1.5 Comprehensive comparison of normal ferroelectrics with relaxor ferroelectrics (adopted from [18]).

(b) Temperature Dependence of Polarization

- Normal Ferroelectrics: The left panel in Figure 1.5 (b) shows a sharp drop in polarization (P_s or P_r) at the T_C, beyond which no polar domains exist. This discontinuity is indicative of a first-order phase transition and is continuous for second order phase transition. At the Curie temperature (T_C), normal ferroelectrics

transition sharply from a paraelectric (non-polar) to a ferroelectric (polar) phase with distinct spontaneous polarization.

- Relaxor Ferroelectrics: The right panel in Figure 1.5 (b) demonstrates a gradual decline in polarization with increasing temperature, extending well above the temperature, T_m (the temperature at which the maximum dielectric constant occurs). Nanoscale polar domains persist above T_m, highlighting the diffuse phase transition characteristic of relaxors. Relaxor ferroelectrics, however, undergo a diffuse phase transition over a broad temperature range due to the gradual formation of PNRs as the temperature decreases.

(c) Dielectric Constant (ε') as a Function of Temperature

- Normal Ferroelectrics: The left panel in Figure 1.5 (c) shows a sharp peak in the dielectric constant at T_C, followed by a rapid decline. The dielectric behavior closely follows the Curie-Weiss law, with minimal frequency dispersion, indicating a narrow and well-defined phase transition.
- Relaxor Ferroelectrics: The right panel in Figure 1.5 (c) displays broad, frequency-dependent peaks in the dielectric constant. These peaks shift with frequency, illustrating strong dielectric dispersion and deviation from the Curie-Weiss behavior. The broad nature of these peaks corresponds to the wide temperature range over which the phase transition occurs, a hallmark of relaxor ferroelectrics. This diffuse transition is associated with the gradual formation and growth of PNRs as the temperature decreases.

(d) Additional Characteristics

Normal Ferroelectrics:

- Sharp, narrow phase transitions with macroscopic symmetry changes at T_C.
- Strong optical anisotropy across T_C.

Relaxor Ferroelectrics:

- No structural phase transition across T_m.
- Critical slowing down of dipolar motion below T_m.
- No optical anisotropy across T_m.

Normal ferroelectrics have a homogeneous microstructure with a regular ion arrangement, leading to consistent polarization and well-defined piezoelectric and pyroelectric properties. Relaxor ferroelectrics, with a heterogeneous microstructure due to random cation distribution, form polar nanoregions (PNRs). This results in enhanced and tunable dielectric and electromechanical properties, such as high electrostrictive and piezoelectric coefficients. They are ideal for high-capacitance multilayer ceramic capacitors (MLCCs), actuators, transducers, and energy harvesting devices. These materials excel in medical ultrasound transducers for high-performance imaging and in energy harvesting applications. Research aims to understand relaxor behavior and improve their properties, focusing on lead-free alternatives like Bi-based relaxors for environmental safety. Advances in thin films and nanostructures are enabling high-performance, miniaturized components for microelectronics.

1.6 Perovskites

Perovskites are a versatile class of materials distinguished by their unique crystal structure and broad range of physical properties. The structure is named after the mineral perovskite (calcium titanium oxide, $CaTiO_3$), discovered by Gustav Rose in 1839 and named after the Russian mineralogist Lev Perovski. The perovskite oxide materials having a general chemical formula of ABO_3 as shown in Figure 1.6, where 'A' and 'B' are

cations of different sizes, and 'O' is an oxygen anion that typically forms bonds with both cations offering a wide range of functional properties. Perovskite structure provides a versatile framework for modifying and enhancing the intrinsic properties of ceramics through various substitutions at the A and/or B sites. This adaptability allows for extensive tailoring of compositions and properties to meet specific operational demands. In contrast, ferroelectric ceramics, especially those based on perovskite structures, offer a cost-effective alternative with significantly higher piezoelectric capabilities.

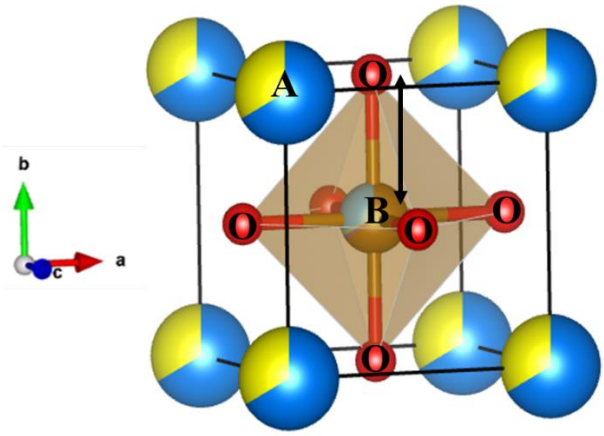

Figure 1.6 Schematic diagram for ideal cubic perovskite structure.

1.6.1 Crystal Structure and Wyckoff Positions

The ideal perovskite structure is cubic and belongs to the Pm3m space group. It can be conceptualized as a network of corner-sharing BO_6 octahedra, with the 'A' cation occupying the interstitial sites between the octahedra.

- A-site cations occupy the (0, 0, 0) positions at the 1 (a) Wyckoff site.

- B-site cations are located at the (1/2, 1/2, 1/2) positions at the 1 (b) Wyckoff site.

- O anions are positioned at (0, 1/2, 1/2) at the 3 (d) Wyckoff site.

This arrangement results in a highly symmetric and stable cubic structure. However, various distortions can lead to lower symmetry structures (tetragonal, orthorhombic, or rhombohedral), depending on the specific ions occupying the A and B sites and external conditions such as temperature and pressure.

1.6.2 Coordination and Site Preferences

In the perovskite structure, the 'A' cation is typically larger and exhibits a 12-fold coordination, indicating it is surrounded by 12 oxygen ions in a cuboctahedral arrangement. This cation generally has a lower charge and is often an alkali or alkaline earth metal such as Na^{+}, K^{+}, Ca^{2+}, or Sr^{2+} [19]. The 'A' cation is situated at the corners of the cubic unit cell. Conversely, the 'B' cation, which is smaller, possesses a 6-fold coordination, being surrounded by six oxygen ions in an octahedral configuration. This cation tends to have a higher charge, commonly found in transition metals like Ti^{4+}, Mn^{4+}, Fe^{3+}, Ta^{5+}, Ga^{3+}, or Nb^{5+}, and is located at the centre of the cube [19]. The oxygen anions are positioned at the face centres of the cube, coordinating with the 'B' cation to form the characteristic octahedral structure.

The allocation of ions to the 'A' or 'B' sites in a perovskite structure is predominantly determined by their ionic sizes and valences. Larger ions with lower charges are typically accommodated at the 'A' site due to its higher coordination number, whereas smaller, highly charged ions prefer the 'B' site because of the octahedral environment. Computational methods and empirical rules, such as the tolerance factor, are often employed to predict and validate these site preferences.

A critical parameter in determining the stability and formation of the perovskite structure is the Goldschmidt tolerance factor (t), defined as [19]:

$$t = r_A + r_B/\sqrt{2}(r_B + r_O) \qquad (1.7)$$

where r_A, r_B and r_O are the ionic radii of the 'A' and 'B' cations and oxygen anion, respectively.

- When t is close to 1, the perovskite structure is typically stable and cubic.

- If t < 1, the structure tends to distort to accommodate the smaller 'A' cation, leading to lower symmetry structures (tetragonal or orthorhombic).

- If t > 1, the structure may become too strained, often leading to hexagonal or other non-perovskite structures.

The tolerance factor thus provides insight into the likely geometry and stability of the perovskite material. Furthermore, the versatility of the perovskite structure arises from its ability to undergo various unit cell distortions. These distortions can occur along different crystallographic directions: [100] direction (cube edges) resulting in a tetragonal cell, [110] direction (cube face diagonal) leading to an orthorhombic cell, [111] direction (cube volume diagonal) creating a rhombohedral cell, and arbitrary [hk0] or [hkl] directions producing monoclinic and triclinic cells, respectively. These distortions often involve the tilting of oxygen octahedra, which forms glide mirror planes within the structure. In the cubic configuration, the three equivalent [100] directions allow for spontaneous polarization in six possible directions: ±[1,0,0], ±[0,1,0], and ±[0,0,1]. This results in 12 potential domain variants in the orthorhombic structure, 8 in the rhombohedral structure, 24 in the monoclinic structure, and 48 in the triclinic structure [4], [20].

1.6.3 Properties of Perovskite Oxides

Perovskite oxides exhibit a diverse range of properties, rendering them highly versatile for numerous applications. These properties can be broadly categorized into electronic, ferroelectric, piezoelectric, magnetoresistive, optical, and ionic conductivity domains.

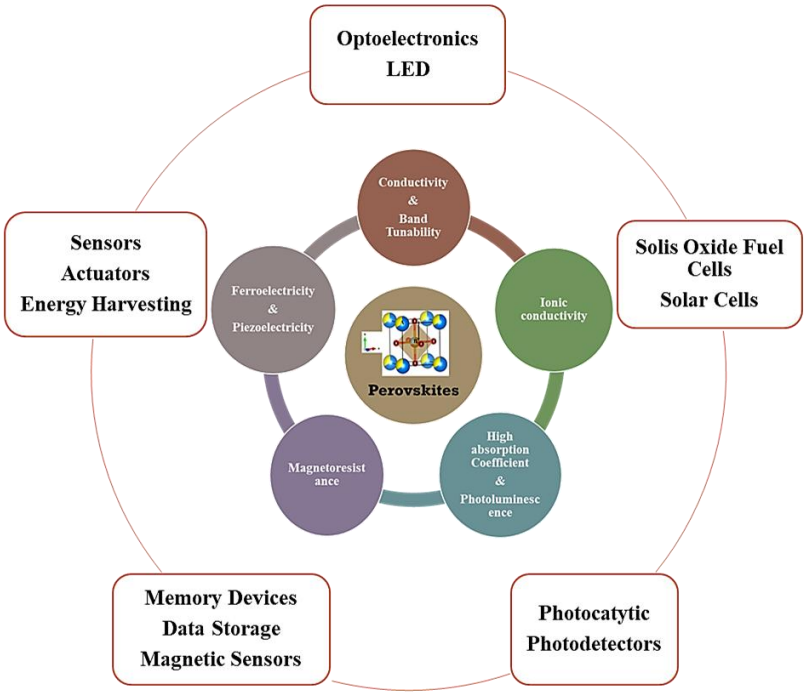

Figure 1.7 Key properties and applications of perovskites.

1.6.3.1 Electronic Properties

1. Conductivity:

Perovskites can exhibit metallic, semiconducting, or insulating behavior depending on their composition and the valence states of the 'A' and 'B' cations. For instance, perovskites like strontium titanate ($SrTiO_3$) function as semiconductors, whereas others such as lanthanum nickelate ($LaNiO_3$) demonstrate metallic properties. Doped perovskites like lanthanum strontium manganite (LSMO, $La_{(1-x)}Sr_xMnO_3$) are noteworthy for their colossal magnetoresistance, a phenomenon where the material's electrical resistance undergoes a substantial change in response to an applied magnetic field. Additionally, barium titanate ($BaTiO_3$) is recognized for its ferroelectric properties.

2. Bandgap Tunability:

The bandgap of perovskites can be precisely controlled by modifying their composition, thereby tailoring their electronic and optical properties. This tunability is particularly advantageous for photovoltaic applications, where bandgap engineering is essential for optimizing light absorption and charge carrier dynamics. The ability to adjust the bandgap facilitates the development of materials with specific properties suitable for various electronic devices.

3. Ferroelectricity and Piezoelectricity

Certain perovskites, such as $BaTiO_3$ and PZT exhibit ferroelectric and piezoelectric properties. These materials possess a spontaneous electric polarization that can be reversed by applying an external electric field. Such characteristics are invaluable in the development of memory devices, sensors, and actuators. The reversible polarization in these materials underpins their functionality in applications requiring precise control of electric fields.

4. Magnetoresistance

Perovskites such as LSMO exhibit colossal magnetoresistance, where the electrical resistance of the material changes significantly in the presence of a magnetic field. This property is harnessed in various applications, including magnetic sensors and data storage devices, where changes in resistance can be utilized for detecting magnetic fields or storing information.

1.6.3.2 Optical Properties

1. High Absorption Coefficients:

Perovskites possess strong absorption coefficients in the visible spectrum, making them highly effective for light harvesting in thin-film solar cells. Their excellent light

absorption properties enable the efficient conversion of sunlight into electrical energy, contributing to the advancement of renewable energy technologies.

2. Photoluminescence:

Many perovskites exhibit robust photoluminescence, which makes them suitable for applications in light-emitting diodes (LEDs) and display technologies. Their ability to emit light efficiently under electrical excitation is exploited in the development of high-performance lighting and display solutions.

1.6.3.3 Ionic Conductivity

Certain perovskites, such as yttria-stabilized zirconia (YSZ), exhibit excellent ionic conductivity, making them suitable for use in solid oxide fuel cells (SOFCs) and oxygen sensors. The high ionic conductivity of these materials facilitates the efficient transport of ions, which is critical for the performance of fuel cells and the accurate detection of oxygen levels in various environments.

Perovskite oxides are a highly versatile class of materials with adaptable structures and multifaceted properties, including electronic, ferroelectric, piezoelectric, magnetoresistive, optical, and ionic conductivity. Their ability to accommodate a wide range of ions and exhibit diverse properties makes them suitable for numerous advanced technological applications. Ongoing research aims to address challenges related to their stability and environmental impact, paving the way for their widespread use in energy and electronic devices. Continued exploration of perovskite materials promises further advancements in materials science and engineering, solidifying their role in future technologies.

1.7 Transition to Lead-Free Piezoelectric Materials: Enhancing Sustainability and Mitigating Health Risks

Transitioning to lead-free piezoelectric materials is crucial for enhancing sustainability and mitigating the significant environmental and health risks posed by lead-based materials like PZT. The inherent toxicity of lead, evident throughout its lifecycle from production to disposal, poses severe risks including developmental and neurological damage, particularly to children, and widespread environmental degradation. These risks are exacerbated by lead smelting and the improper disposal of electronic waste, which releases toxic substances into ecosystems, contributing to soil and water contamination.

1. Lead Toxicity and Health Risks:

- General Toxicity: PZT, widely used in various industries, contains lead, a toxic element that poses serious risks throughout its lifecycle, including production and disposal. Lead's toxicity adversely affects multiple bodily systems and can lead to severe health problems [20], [21], [22].
- Effects on Children: Lead is particularly harmful to children, impairing cognitive development, reducing intelligence, shortening attention span, and decreasing academic performance. Even low levels of exposure can have significant impacts. Children living near e-waste processing sites are at high risk of lead poisoning, which can cause developmental and neurological damage.
- Chronic Health Conditions: Elevated lead exposure is associated with anemia, hypertension, renal impairment, and damage to reproductive organs. The neurotoxic and behavioral impacts of lead are often irreversible, necessitating stringent measures to minimize its use in consumer products.

2. Occupational and Environmental Hazards:

- Inhalation Risks during Manufacturing: During the manufacturing process of lead-based piezoelectric materials, workers are at risk from inhaling lead oxide dust and vapors, posing significant health risks. Adopting lead-free ceramics can significantly mitigate these health risks.
- Environmental Contamination: The extraction and processing of lead contributes to substantial environmental degradation. Lead smelting releases large quantities of lead and cadmium into the atmosphere, affecting local ecosystems and leading to widespread soil and water contamination. By eliminating lead from the production process, lead-free ceramics reduce the environmental burden associated with lead mining and refining.
- Disposal and E-Waste Concerns: Improper disposal of lead-based products, especially in electronic waste, exacerbates environmental contamination. E-waste frequently ends up in landfills or is improperly recycled, leading to lead leaching into the environment and posing serious health risks to nearby communities. These effects are particularly severe in developing countries where environmental regulations may be less stringent. Recycling and disposing of lead-free materials are more manageable, supporting circular economy principles. Thus, the transition to lead-free piezoelectric materials is not only essential for mitigating environmental and health impacts but also pivotal for advancing sustainable technologies and energy solutions.

3. Regulatory Imperatives:

- Need for Regulation: The well-documented dangers of lead underscore the necessity for stringent regulations to control its use and to promote safer alternatives in the production of consumer products.
- Global Regulations and Standards: Efforts such as the European Union's RoHS directive aim to mitigate the environmental and health impacts of hazardous substances like lead by restricting their use and encouraging the development of lead-free alternatives. Lead-free alternatives, such as KNN, offer promising replacements for PZT. Although the transition involves overcoming challenges related to material properties and production scalability, the benefits of reduced lead exposure and environmental contamination are substantial. Continued research and development in lead-free piezoelectric materials are essential for achieving safer and more sustainable solutions.

Despite the technical and cost challenges associated with transitioning to lead-free materials, the long-term benefits of reduced lead exposure justify these efforts. More specific details on can be found in the article "Lead-free piezoelectrics—The environmental and regulatory issues" by Andrew J. Bell and Otmar Deubzer [23]. Ongoing research and supportive legislation are essential for overcoming these challenges, making the adoption of lead-free ceramics in various applications a crucial step toward a safer and cleaner future.

1.8 Foundational Perspective on Phase Boundaries

1.8.1 Morphotropic Phase Diagram (MPB)

MPBs are critical regions in the phase diagram of certain piezoelectric materials where two or more crystallographic phases coexist. These boundaries are driven by composition rather than temperature or pressure, and they play a significant role in enhancing the

piezoelectric properties of materials. The MPB is characterized by a sharp change in crystal structure, leading to improved electromechanical coupling and higher piezoelectric coefficients. However, it was the discovery of MPBs in PZT ceramics during the 1950s that highlighted their importance [15]. In PZT, the highest piezoelectric properties were observed at a composition near the MPB between the rhombohedral and tetragonal phases, specifically at a Zr/Ti ratio of approximately 52:48 [24]. This discovery has driven extensive research into the phase boundary engineering of piezoelectric materials. The enhanced piezoelectric properties at MPBs result from several key mechanisms. First, the coexistence of different phases at MPBs facilitates easy rotation of the polarization vector, significantly improving the material's response to an external electric field and resulting in higher piezoelectric constants [25]. Second, increased domain wall mobility at MPBs enhances the overall piezoelectric response. Domain walls can move more easily within the flattened energy landscape, facilitating polarization switching. Lastly, near the MPB, the Gibbs free energy profile exhibits significant flattening, indicating minimal free energy differences between the competing phases. This flattening is crucial for piezoelectric performance as it lowers the energy barrier for polarization rotation, allowing the polarization vector to reorient easily under an external electric field, resulting in a large piezoelectric response. The coexistence of multiple phases at the MPB facilitates smooth transitions between them, enabling optimization of material properties by tailoring composition and external conditions. By precisely controlling the composition and processing conditions to position materials near their MPB, researchers can achieve superior piezoelectric performance. In summary, the instability and flattening of the Gibbs free energy profile near the MPB are fundamental to developing high-performance piezoelectric materials. The study of MPBs has led to significant advancements in both lead-based and lead-free piezoelectric materials,

providing a pathway for optimizing material performance for various applications. These insights guide both theoretical research and practical applications in materials science, making MPBs critical for optimizing piezoelectric performance.

1.8.2 Phase Boundaries in Lead-Based and Lead-Free Piezoelectric Perovskite Materials

Phase diagrams are essential tools in materials science, providing critical information about the stability and transformations of different phases under varying conditions of temperature, pressure and composition. They are particularly useful in understanding the phase relationships in perovskite systems, guiding the synthesis and optimization of materials with desired properties. Phase boundaries are inherent components of phase diagrams which play a crucial role in enhancing the electrical properties of both lead-based and lead-free piezoelectric perovskite materials. In 1952, Shirane et al. investigated the solid solution of $(1-x)PbZrO_3$-$xPbTiO_3$ for the first time [26]. Further building upon this, Jaffe et al. constructed the phase diagram for $(1-x)PbZrO_3$-$xPbTiO_3$ solid solution where they found MPB at Zr/Ti ratio of 52:48 which resulted in the highest piezoelectric constant, d_{33} as shown in Figure 1.8 [4], [24]. This specific composition leads to the formation of a rhombohedral-tetragonal (R-T) MPB, which is widely regarded as a classic example of optimizing piezoelectric performance. Although there are some discrepancies regarding the phase boundaries in PZT, as in 1999, Noheda et al., discovered monoclinic phase between previously reported R-T phase boundary using high resolution Synchrotron XRD [27]. Later it was supported by first principle calculations that monoclinic phase serves as the bridge between R-T phase boundary with the high piezoelectricity attributed to facilitated polarization rotation due to the presence of the monoclinic phase as it offers increased no. of polarization directions [28].

In 2009, Damjanovic et al. offered a different perspective on the origins of the enhanced piezoelectric properties in ferroelectrics, based on theoretical and experimental evidence [29]. They emphasized the role of polarization rotation and monoclinic phases but argued that the highest piezoelectricity is often observed in phase transition regions where polarization changes direction or emerges from a nonpolar state, rather than being directly related to monoclinic phases. Consequently, debates about the intermediate phase in PZT continue. The type of phase boundary significantly influences the corresponding piezoelectric activity. In lead-free piezoelectric perovskite materials, similar enhancements in piezoelectric response have been observed in compositions that exhibit an R-T phase boundary [4], [30], [31]. These materials show a higher piezoelectric response compared to those with other types of phase boundaries. This phenomenon underscores the importance of phase boundary engineering in the development of high-performance piezoelectric materials.

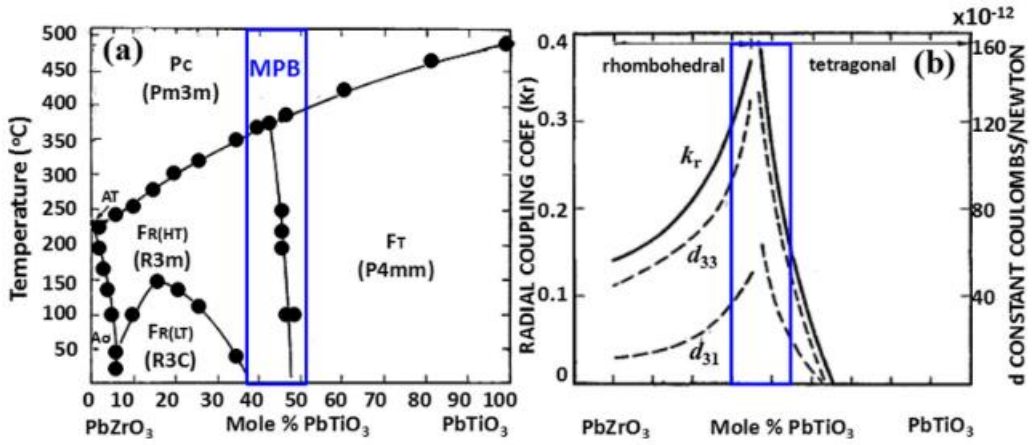

Figure 1.8 (a) Phase diagram and (b) Composition dependent planar coupling coefficient and piezoelectric coefficients of (1-x)$PbZrO_3$-x$PbTiO_3$ solid solution (adopted from [4], [15], [24]).

Apart from experimental investigations, theoretical frameworks, such as the Landau phenomenological theory and first-principles calculations, have been instrumental in

understanding phase transitions in piezoelectric materials. These theories were extensively used in the 20th century to elucidate the mechanisms underlying phase transitions from a theoretical perspective [25], [32], [33]. The core concept in Landau theory is the Gibbs free energy, which varies with temperature, composition, electric field, and other external parameters [34]. Thus, the relationship between phase boundaries, Gibbs free energy, and piezoelectric properties is therefore critical and is further discussed in the following section. Understanding and manipulating this relationship can lead to substantial improvements in the performance of piezoelectric materials.

Landau phenomenological theory and first-principles calculations provide the theoretical basis for explaining phase transitions in piezoelectric materials. The Landau theory focuses on the dependency of Gibbs free energy on external parameters, leading to a better understanding of the phase boundary effects. It describes phase transitions by introducing an order parameter, which changes its value during the transition. For piezoelectric materials, the order parameter is often the polarization (P). Landau free energy in one dimension can be given by below expression:

$$\boldsymbol{F(P,T)} = \left(\frac{\mathbf{1}}{\mathbf{2}}\right)\boldsymbol{\alpha P^2} + \left(\frac{\mathbf{1}}{\mathbf{4}}\right)\boldsymbol{\beta P^4} + \left(\frac{\mathbf{1}}{\mathbf{6}}\right)\boldsymbol{\gamma P^6} + \ldots\ldots \qquad (1.8)$$

where α, β, and γ are temperature dependent coefficient. The odd powers in the above expansion are omitted as on considering even powers the free energy will not change on polarization reversal ($\boldsymbol{P} \rightarrow -\boldsymbol{P}$). The detailed mathematical description for the same can be found elsewhere [34], [35]. Near the MPB, the free energy profile becomes flat, indicating near-degeneracy of phases as shown in Figure 1.9. First-principles calculations, particularly those based on density functional theory (DFT), provide an atomistic insight into the electronic and structural properties that drive phase transitions by solving the fundamental equations of quantum mechanics. These calculations provide

detailed insights into the electronic and structural mechanisms underlying these transitions. Combining Landau theory with first-principles calculations provides a comprehensive understanding of phase transitions and enables the design and optimization of high-performance piezoelectric materials [36].

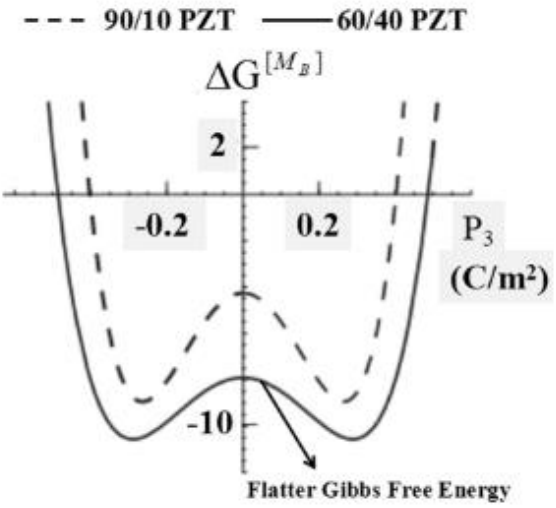

Figure 1.9 A cross-sectional analysis of the Gibbs free energy for $Pb(Zr_{1-x}Ti_x)O_3$ compositions with 90/10 and 60/40 ratios along the [M_B] path (adopted from [4], [25]).

1.9 Recent development in Bi-based lead-free piezoceramics

Lead-free piezoelectric ceramics have gained significant limelight due to their potential for superior properties, including high piezoelectric charge coefficient, high T_C, and dielectric permittivity, enabling their use in various multidimensional applications such as actuators, sensors, piezoelectric energy harvesters, energy storage, photovoltaics, and transformers [37], [38], [39], [40], [41], [42]. In contrast to lead-based piezoelectric ceramics, which pose environmental and health concerns due to their high toxicity [23], the European Union's RoHS has driven the efforts to develop new lead-free alternatives for contemporary lead-based piezoceramics [37], [43], [44]. Lead-free piezoceramics can be broadly classified into two main categories: the first category comprises perovskite-structured materials such as KNN, BNT, and BT-based compounds, which are developed

to compete directly with PZT in various applications. This group currently dominates the research landscape for lead-free materials [1], [4], [6], [7], [8], [9], [20], [21], [22], [45], [46], [47], [48], [49]. However, the relatively low T_C of KNN (around 415 °C) and BT (around 120 °C), as well as the low depolarization temperature (approximately 100 °C) of BNT, restrict their use in high-temperature applications. The second category includes materials with properties that PZT cannot match, such as single crystals of SiO_2, AlN, and $LiNbO_3$, tungsten-bronze structured ceramics, Bi-based layer structured ferroelectrics (BLSFs), and high-temperature piezoelectrics like BFO-based ceramics [50]. Each class particularly KNN-based, BT-based, BNT-based, and BFO-based materials, has its own advantages and disadvantages depending on the intended application [43], [51], [52], [53], [54], [55], [56], [57]. For high-temperature applications that require operation under elevated temperatures (e.g., space exploration, nuclear reactors, fuel injectors, and oil drilling), materials capable of withstanding temperatures as high as 300 °C or even higher are necessary [58], [59]. Bismuth, a non-toxic heavy metal, is particularly noteworthy as studies have shown it has negligible harmful effects on living organisms, making bismuth-based ceramics an attractive option for environmentally friendly piezoelectric materials [60], [61]. The enduring dominance of lead-based piezoceramics, especially PZT, in the piezoelectric market for over half a century is due not only to their exceptional properties but also to their cost-effectiveness, as most commercially available lead-based piezoceramics, like PZT, PMN-PT, and PLZT, are derived from relatively inexpensive raw materials, as illustrated in Figure 1.10. Moreover, achieving a high density (over 96%) of raw materials is easily attainable through conventional pressure less sintering techniques, making economic considerations as crucial as functional properties in the development of lead-free piezoceramics. The affordability and safety of bismuth-based materials highlight their significance in the

pursuit of lead-free piezoceramics, offering a viable, non-toxic alternative to traditional lead-based options. High-temperature lead-free Bi-based piezoceramics can be categorized into three distinct groups, as shown in Figure 1.11. The first group includes BFO-based ceramics, known for their multiferroic properties. The second group consists of BNT-based ceramics, recognized for their high piezoelectric strain coefficient, making them potential candidates for actuator applications. The third group comprises Aurivillius-based ceramics, with a particular focus on Bismuth Titanate ($Bi_4Ti_3O_{12}$ or BIT), known for their high Curie temperature (T_C) and high-temperature piezoelectric properties. Each of these categories represents different types of lead-free Bi-based piezoceramics, offering unique properties and applications, particularly suitable for high-temperature environments. Further sections will discuss each class in detail.

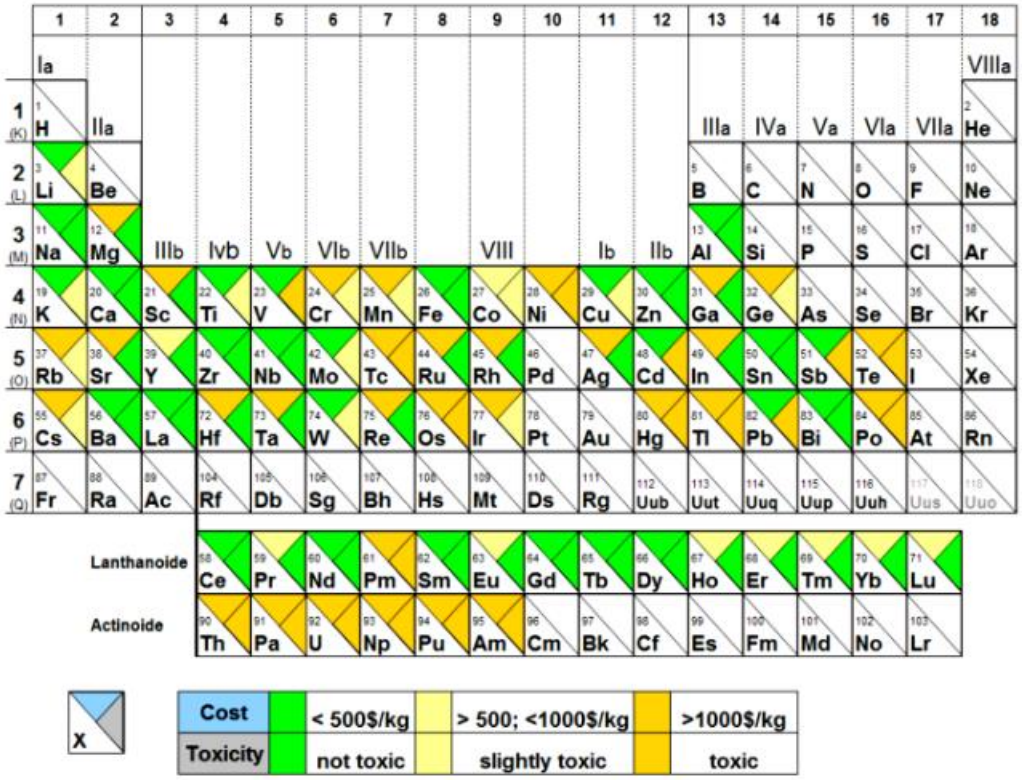

Figure 1.10 Differentiation of elements based on toxicity and cost (adopted from [20]).

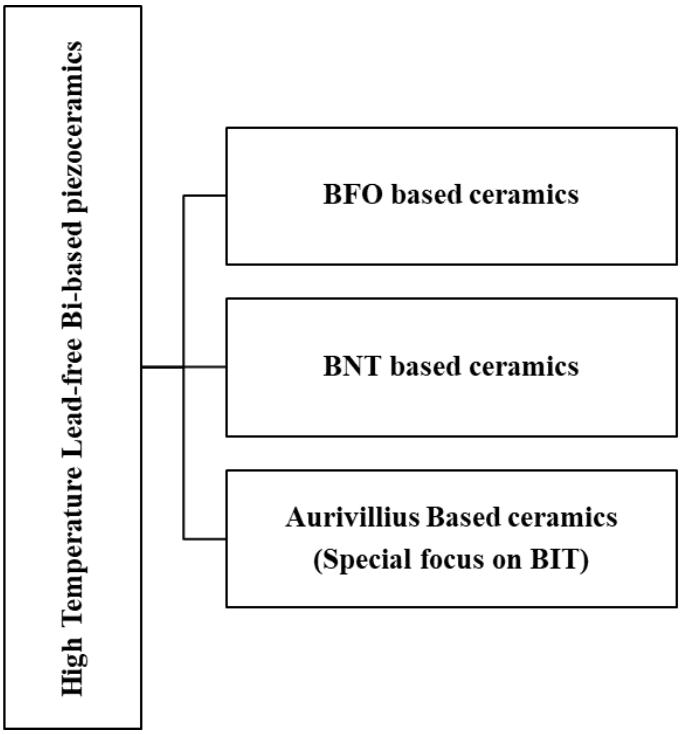

Figure 1.11 A broad classification of high temperature lead-free Bi- based piezoelectric materials.

1.9.1 $BiFeO_3$ (BFO) Based Piezoceramics

BFO has garnered significant attention since its discovery due to its unique multiferroic properties, exhibiting both ferroelectric and antiferromagnetic characteristics at room temperature [62]. BFO possesses a distorted rhombohedral perovskite structure with the R3*c* space group at room temperature [16], [63]. This non-centrosymmetric structure is crucial for its ferroelectric properties. $BiFeO_3$ exhibits high polarization (P_s~ 90-100 μC/cm² at room temperature) and a high T_C (~830 ℃), which makes it suitable for high-temperature applications with potential for offering additional functionalities [16], [64], [65]. Additionally, it has a G-type antiferromagnetic order with a Néel temperature around 370 ℃, further enhancing its appeal in multifunctional device applications. However, despite its improved properties, the practical use of BFO-based ceramics is hindered by several limitations, such as difficulties in achieving pure phase formation,

reduction of Fe- valence state, challenging poling due to large leakage current losses, thermodynamic instability in intermediate temperature ranges, and the creation of defect oxygen vacancies required to maintain charge neutrality [43], [66], [67]. Researchers have been employing site engineering as a strategy to overcome these issues of BFO and promote the desired ferroelectric, magnetic, and piezoelectric properties in bulk ceramic form by suitable substitution at the A and/or B sites, which can also help improve resistivity by reducing leakage current [68], [69], [70], [71], [72], [73], [74]. Doping Bi-site with rare-earth elements ions like La, Nd, Dy, Y, Ce, Eu, Yb, Pr and Sm has been instrumental in enhancing the piezoelectricity and ferroelectricity [64], [75], [76], [77], [78], [79]. For instance, a high d_{33} ~ 50 pC/N and low leakage characteristics were obtained for Sm, La modified BFO [80]. The enhancement in the electrical properties is commonly attributed to reduction in leakage current and suppression of secondary phase formation. These dopants have been shown to reduce leakage current, improve polarization, and enhance magnetoelectric coupling. Ion substitution at Fe site by transition metals like Mn, Co, Sc, Ta, and Ti has been widely researched but does not deliver desired properties [4], [64]. Although in case of Sc doped BFO, enhanced electrical properties were reported (d_{33}~46, P_r~15 μC/cm^2) [81]. $BiFeO_3$-based piezoceramics offer several advantages, including their multifunctionality due to the coexistence of ferroelectric and antiferromagnetic properties. However, several drawbacks limit the practical application of $BiFeO_3$. High leakage current and large coercive fields resulting from intrinsic defects, reduction of Fe, oxygen vacancies and the volatility of bismuth poses a significant challenge. Additionally, despite the coexistence of electric and magnetic orders, the magnetoelectric coupling in BFO is relatively weak. Furthermore, the difficulty in synthesis, requiring precise control over stoichiometry and defects, complicates large-scale production. Improving the electrical properties of BFO

ceramics through ion substitution is challenging because of the absence of phase boundaries, limiting their effectiveness (d_{33}≤50 pC/N) [79], [81]. To address this, researchers have explored forming its solid solution formation with other ABO_3-type perovskites which has proven to be an effective strategy for significantly enhancing electrical and magnetic properties at higher temperatures [82], [83], [84]. Two common additions are $BiFeO_3$-$PbTiO_3$ and $BiFeO_3$-$BaTiO_3$ (BF-BT) [85], [86], [87], [88]. $BiFeO_3$-$PbTiO_3$ can achieve good piezoelectricity by creating a phase boundary, but it contains lead, which is hazardous, so it hasn't been widely adopted. Other ABO_3 materials have also been tested to enhance BFO ceramics' electrical properties, but these combinations often result in high leakage currents, leading to poor ferroelectric and piezoelectric properties. Examples include $BiFeO_3$ combined with $SrTiO_3$, $CaTiO_3$, $NaNbO_3$, KNN, and $Bi_{0.5}K_{0.5}TiO_3$ [4], [30], [89], [90], [91]. PZT and BF-BT solid solutions both transition from R to T structures as BT and PT concentrations increase. However, in BF-BT, both A-site and B-site are occupied by multiple ions, unlike PZT, where only the B-site has multiple ions. In PZT, Ti and Zr influence the displacement of Pb's lone pair electrons, whereas in BF-BT, Ba blocks Bi displacements, and Fe competes with Ti on the B-site. This competition creates a tendency for short-range ordered pseudosymmetric structures, resulting in broader relaxor-like dielectric behavior. While BF-BT may not achieve large piezoelectric coefficients (d_{33}), it exhibits a high strain electrostrictive response, making it suitable for high energy density storage, electrocaloric, and pyroelectric applications.Also compared to BF-PT, the lead-free BF-BT system is more appealing due to its superior piezoelectric performance and relatively high T_C exceeding 400°C due to which the focus has shifted to developing BF-BT based systems, which shows promise for better electrical properties and is discussed in detail in the next section.

1.9.1.1 Evolution and Recent Development of $BiFeO_3$-$BaTiO_3$ (BF-BT) System

In BFO, the ferroelectricity arises from the lone pair electrons in the Bi 6s orbital, while the magnetic moment is due to the partially filled d orbitals of Fe. Consequently, appropriate chemical modifications at both sites can enhance the ferroelectric, piezoelectric and magnetic properties. As discussed in previous section addition of ABO_3 type end member helps in enhancing the functional properties. Since $BaTiO_3$ (BT) is recognized for its ferroelectric characteristics and has a relatively low T_C [92]. Although this low T_C initially raised concerns for its use in high-temperature applications for BT but the outstanding dielectric and ferroelectric properties, tetragonal structure at room temperature, and lead-free composition make it a suitable choice to enhance the inadequate dielectric and ferro-piezoelectric properties of BF. In 2009, Liu and Ren found that Ca- and Zr-modified BT (BCZT) exhibited remarkable piezoelectric properties, sparking renewed research into lead-free piezoelectrics [93]. BCTZ exhibits a tricritical point where cubic, tetragonal, and rhombohedral structures coexist, achieving ultrahigh piezoelectricity of 620 pC/N [93]. The energy profile near this triple point favors polarization rotation, which is key to its exceptional piezoelectricity. In another study in 2020, Wang and others reported an exceptional d_{33} exceeding 1100 pC/N in Sn-doped $BaTiO_3$ BTSx (x= 0.11) ceramics, the highest value recorded for lead-free ceramics as depicted in Figure 1.12 [94]. This remarkable increase in piezoelectricity was due to the strategic design of a flat Gibbs free energy density profile, accomplished through a combined approach involving the coexistence of multiple phases and local structural heterogeneity. Although subsequent BT-based piezoelectrics demonstrated excellent piezoelectric properties, they were typically limited to a narrow temperature range. BT has been extensively studied for various factors, including grain size effect, crystal structure, nanoparticles, and texturing. Despite these advancements, the low Curie

temperature (<130 °C) of BT-based systems remain a significant limitation for their practical use in devices.

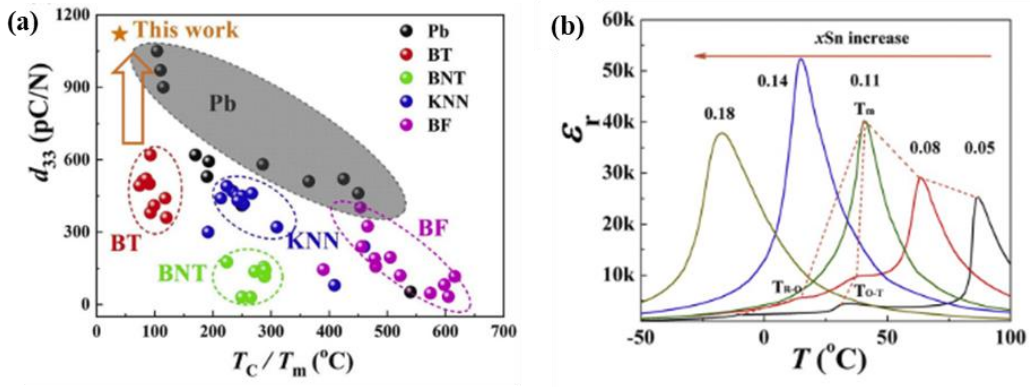

Figure 1.12 (a) d_{33} vs T_C/T_m comparison for piezoelectric ceramics with max d_{33} obtained for Sn doped BT (BTSx, x=0.11) (b) Temperature dependent dielectric permittivity for BTSx with respect to Sn content (adopted from [94]).

In 1964, Venevtsev et al. discovered that the BF-BT system forms a continuous solid solution at room temperature, with three different crystal structures: R for compositions ranging from 100-67% BF, pseudocubic for 67-7.5% BF, and T for 7.5-0% BF. This was later validated by Kumar et al. [95]. The solid solution of (1-x)BF-xBT system exhibits several structural transitions throughout its compositional range, typically influenced by the concentration of BT. At room temperature, a rhombohedral phase is stable for low concentrations of BT ($x < 0.3$), which transforms to a pseudocubic phase around x~0.33 and becomes tetragonal when the BT concentration exceeds 92% [44], [96], [97]. In 2009, Leontsev and Eitel presented a revised phase diagram for the solid solution of (1-x)BF-xBT as demonstrated in Figure 1.13 (a), earlier given by Kumar et al. revealing the existence of a MPB within a specific composition range of $0.25 < x < 0.4$, spanning the transition between rhombohedral and cubic phases [95], [98]. The accelerated research in search of MPB can be understood by the fact that generally piezoelectric properties get enhanced in its vicinity [99]. They reported piezoelectric charge coefficient, d_{33} value of

approximately 116 pC/N, T_C of around 620 °C, and a depolarizing temperature surpassing 400 °C for MnO_2-modified $BiFeO_3$-$BaTiO_3$ (BF-BT) solid solution with 22-40 mol % BT content [100].

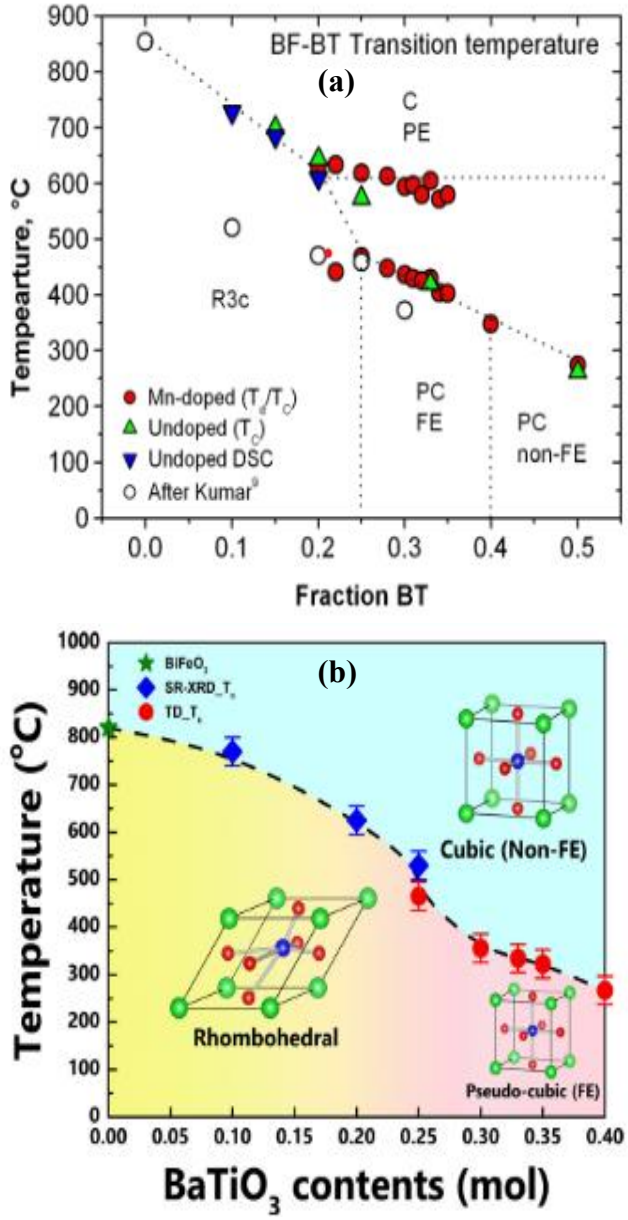

Figure 1.13 Revised phase diagram of BF-BT solid solution by (a) Leontsev et al. after Kumar [95] et al. (adopted from [98]) and (b) Kim et al. after carrying out synchrotron XRD and temperature dependent dielectric properties measurement (adopted from [101]).

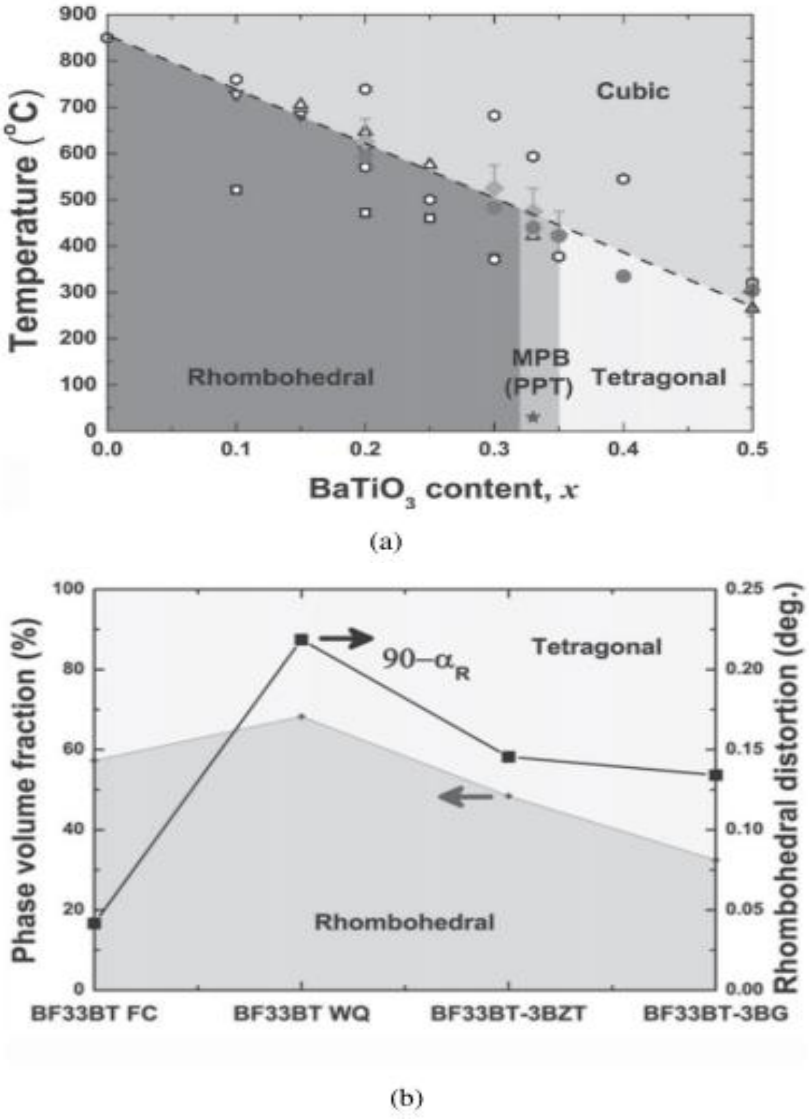

Figure 1.14 (a) Phase diagram of BF-BT solid solution and (b) Rhombohedral distortions (90°-α_R) and phase volume fractions of furnace-cooled BF33BT FC, water-quenched BF33BT WQ, BF33BT-3BZT, and BF33BT-3BG ceramics (adopted from [31]).

In 2014, Lee et al. reported modified phase diagram with R-T MPB having highest till date d_{33} value of ~402 pC/N and T_C of ~454 ℃ for water quenched 0.67($BiFeO_3$)-0.33($BaTiO_3$)-3 mol % $BiGaO_3$ piezoelectric ceramic as shown in Figure 1.14 and Figure 1.15 respectively, although subsequent reproducibility of these results has been challenging [102]. This discrepancy is likely due to the sensitivity of the physical

properties of BF-based materials to their crystal symmetry and microstructure (e.g., compositional inhomogeneity and core-shell structure), which are influenced by experimental procedures such as annealing and quenching, resulting in varying piezoelectric performance. In 2017, Kim et al. proposed a phase diagram for the BF-BT system based on the analysis of electrical properties, the published T_C of BF, and temperature-dependent SR-XRD profiles, as shown in Figure 1.13 (b). While previous phase diagrams indicated a transition from a ferroelectric (FE) pseudo-cubic to a non-ferroelectric (non-FE) pseudo-cubic structure at BF35BT, this study observed good electrical properties in BF40BT, suggesting an FE pseudo-cubic structure for BFxBT with x = 0.30–0.40.

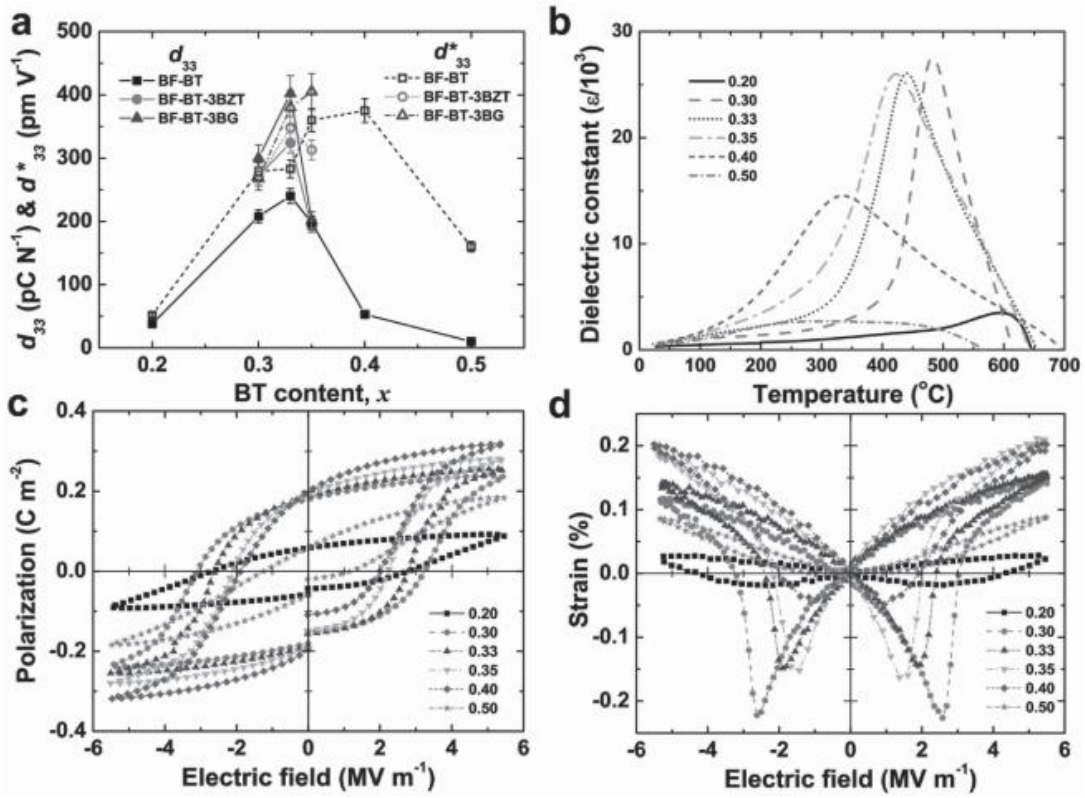

Figure 1.15 (a) d_{33} and d_{33}^* values of 0.67BFO−0.33BTO (BF33BT), 0.7(BF33BT)−0.3Ba($Zr_{0.5}Ti_{0.5}$)O_3 (BF33BT-3BZT) and 0.7(BF33BT)−0.3$BiGaO_3$ BF-BT-3BG as function of BT content (b) temperature dependent dielectric constant of BF-BT ceramics (c) P-E loops of BF-BT ceramics and (d) bipolar S-E hysteresis loops of BF-BT ceramics (adopted from [31]).

However, accurately determining the phase transformation for compositions with over 30% BT content in the BF-BT system is challenging.

The increased presence of the pseudocubic phase affects both structural and dielectric data during heating and cooling, causing broad peaks in the measurements. Observations from these phase diagrams reveal that the BF-BT solid solution system does not exhibit a specific region or boundary with coexisting R-T symmetries, like the MPB in PZT ceramics. However, the region between 0.67 and 0.75 in the BF-BT system is of particular interest because it shows MPB-like characteristics with rhombohedral and pseudocubic phases, resulting in excellent ferro-piezoelectric performance and a high T_C. Typical saturated ferroelectric P-E hysteresis loops are rarely seen in the unmodified BF-BT system, particularly on the BF-rich side, due to high leakage current. However, Leontsev et al. reported that adding 0.1 wt% MnO_2 to BF-BT ceramics significantly reduced conductivity and produced well-saturated P-E loops. This finding spurred further research, showing that MnO_2 additions from 0.1 to 0.6 wt% effectively suppress high conductivity. Wei and group studied the BF-BT solid solution (1-x)BF–xBT, $0.2 \leq x \leq 0.45$) as shown in Figure 1.15 where they found 0.7BF-0.3BT composition to have a slight rhombohedral distortion , exhibiting the highest P_r of 26.0 μC/cm^2 and d_{33} of 134 pC/N. Compositions with pseudo-cubic symmetry (intermediate phases) display a relaxor-like dielectric anomaly. As the BT content increases, P_r and d_{33} values decrease, with 0.65BF-0.35BT showing 24.8 μC/cm² and 104 pC/N, and 0.55BF-0.45BT showing 8.2 μC/cm² and 5 pC/N [103]. In Figure 1.17 (a), the hysteresis loops transition from hard-type to soft-type with increasing BT content. Well-saturated P-E loops on the BFO-rich side are due to charged point defects from Bi^{3+} volatilization or Fe^{3+} ion coordination transition [101]. The square shape of BF20BT is due to domain wall depinning and stress relaxation during preparation. Figure 1.17 (b) shows butterfly-shaped S−E curves for BFxBT.

Increasing $BaTiO_3$ content reduces negative strain, indicating enhanced domain switching and material softening. The S-E curve of BF20BT indicates a hard-type ferroelectric, while increasing $BaTiO_3$ content suggests a softer nature. BF30BT exhibited 16% strain hysteresis, comparable to soft PZT (PCI151), with a piezoelectric actuator constant of 362.50 pm/V. The Curie temperatures for BF25BT and BF30BT were 465 °C and 356 °C, respectively, higher than those of PZT-5H and PZT4.

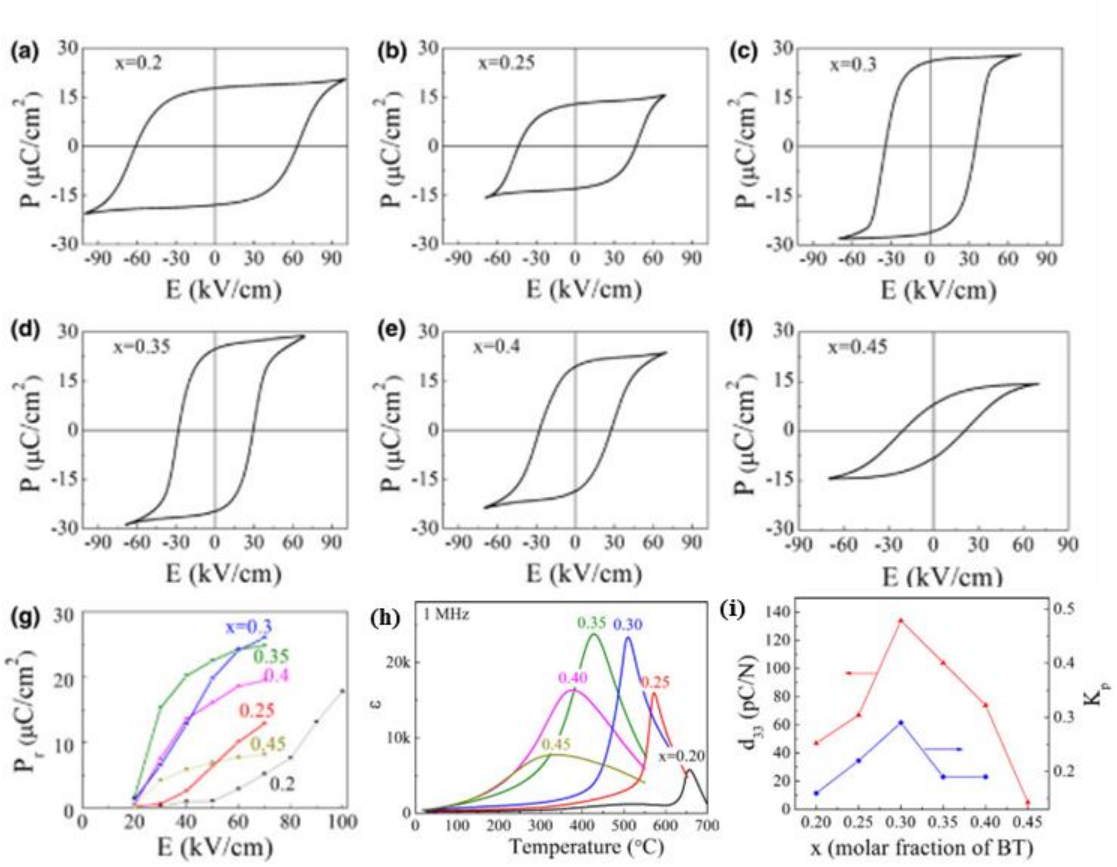

Figure 1.16 (a-f) P-E hysteresis loops for (1-x)BF–xBT, $0.2 \leq x \leq 0.45$), (g) variation of P_r with respect to applied electric field, and (i) d_{33} and electromechanical coupling constant k_p with respect to BT content (adopted from [103]) .

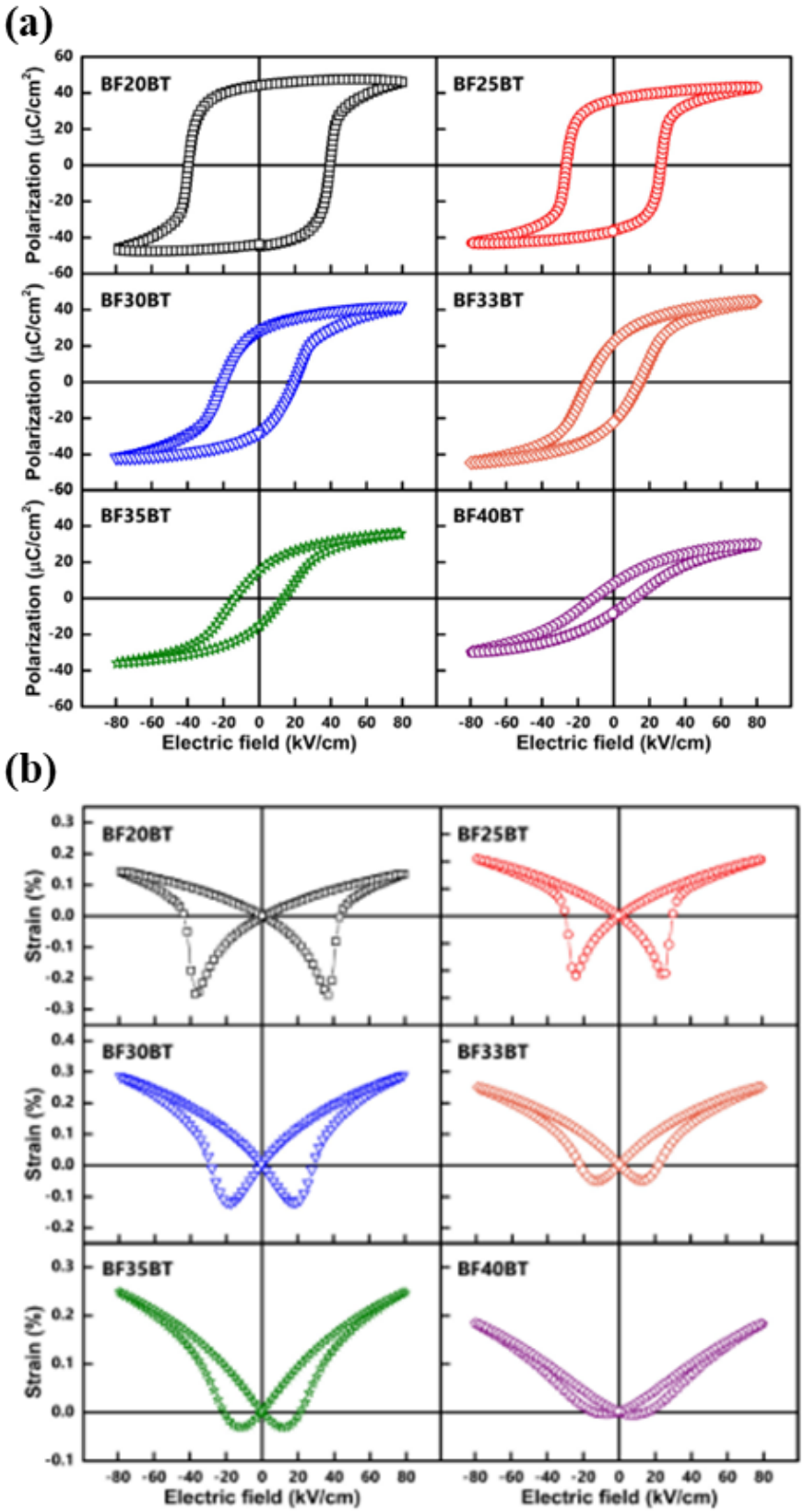

Figure 1.17 (a) Room temperature P-E hysteresis loops measured at 0.1 Hz and (b) Bipolar Strain-Electric field (S-E) loops for BF-BT for BF-BT ceramics with respect to BT concentration (adopted from [104]).

Hence the overall functionality of the BF-BT system can be improved by ion substitution as it can enhance the resistivity, density and promotes the formation of phase boundaries. A table listing the electrical properties of some of the BF-BT based systems is depicted in Table 1.2. Compared to typical ferroelectric materials, relaxor ferroelectric and antiferroelectric materials exhibit higher energy storage efficiency, making them promising candidates for energy storage applications. The BF−BT system is a notable relaxor ferroelectric whose relaxation properties can be tailored by adjusting the BT content. Consequently, there is substantial research focused on BF−BT-based ferroelectric materials [90]. Table 1.3 highlights the electrical parameters of BT−BF-based materials alongside various other lead-free ferroelectric materials.

Table 1.2 Summarizes the electrical properties of differently modified BF-BT systems (adopted from [4]).

Material system	Phase structure	d_{33} (pC/N)	P_r (μC/cm^2)	E_C (kV/cm)	T_C (°C)
$0.8BiFeO_3$–$0.2BaTiO_3$ + SiO_2	R	86			628
$0.8BiFeO_3$–$0.2BaTiO_3(N_2)$	R	98	25.7	74.6	632
$0.75BiFeO_3$-$0.25BaTiO_3$ + MnO_2	R	116	22.9	39.3	619
$0.725BiFeO_3$-$0.275BaTiO_3$	R-Pc	124			
$0.725BiFeO_3$-$0.275BaTiO_3$ + MnO_2	R-Pc	136	15	30	485
$0.70BiFeO_3$-$0.30BaTiO_3$	R-Pc	180	25	23	506
$0.675BiFeO_3$-$0.325BaTiO_3$ + MnO_2 + CuO	R-Pc	170	~20	~30	485
$0.67BiFeO_3$-$0.33BaTiO_3$	R-T	240	~20	~25	456
$0.67BiFeO_3$-$0.33BaTiO_3$ + MnO_2	Pc		39	~25	420
$0.65BiFeO_3$-$0.35BaTiO_3$	Pc	104	30.6	27.9	400
$0.725Bi(Fe_{0.98}Sc_{0.02})O_3$–$0.275BaTiO_3$ + MnO_2	R	127	~20	~50	636
$0.71Bi(Fe_{0.985}Ga_{0.015})O_3$–$0.29BaTiO_3$	Pc	157	8	23	464
$0.71BiFe_{0.994}Co_{0.006}O_3$–$0.29BaTiO_3$	Pc	167			488
$0.75Bi_{0.95}Nd_{0.05}FeO_3$-$0.25BaTiO_3$ + MnO_2	R-M	121	17.5		482
$0.725BiFe_{0.96}Sc_{0.04}O_3$-$0.275BaTiO_3$ + MnO_2	R-M	143	17.6	40	596
$0.72Bi(Fe_{0.99}Al_{0.01})O_3$–$0.28BaTiO_3$	R-Pc	151	14.41	33.31	450
$0.70Bi_{0.98}La_{0.02}FeO_3$-$0.30BaTiO_3$ + MnO_2	R-T	121	25	33	550
$0.70Bi_{1.05}Fe_{0.97}A_{0.03}O_3$-$0.30BaTiO_3$ (A: Sc, Ga, Al)	R-Pc	160–180	18–22	~30	470–500
$0.67Bi_{1.05}Fe_{0.97}Ga_{0.03}O_3$-$0.33BaTiO_3$	R-T	402	20	24	454
$0.97(0.67Bi_{1.05}FeO_3$-$0.33BaTiO_3)$-$0.03Bi_{1.05}(Zn_{0.5}Ti_{0.5})O_3$	R-T	324	24	26	466
$0.715BiFeO_3$-$0.275BaTiO_3$-$0.01Bi(Mg_{0.5}Zr_{0.5})O_3$ + MnO_2	R-T	130	~9	~32	575
$0.705BiFeO_3$-$0.275BaTiO_3$-$0.02Bi_{0.5}Na_{0.5}TiO_3$ + MnO_2	R-T	140	18.4		
$0.725BiFeO_3$-$0.25BaTiO_3$-$0.025Bi_{0.5}K_{0.5}TiO_3$ + MnO_2	R-Pc	134	16.52	4.59	
$0.69BiFeO_3$-$0.29BaTiO_3$-$0.02Bi(Mg_{0.5}Ti_{0.5})O_3$ + MnO_2	Pc	115	24.5	40	509
$0.71BiFe_{0.97}(Mg_{0.5}Ti_{0.5})_{0.03}O_3$-$0.29BaTiO_3$ + MnO_2	Pc	155	~17	~25	425
$0.71BiFe_{0.97}(Ni_{0.5}Ti_{0.5})_{0.03}O_3$-$0.29BaTiO_3$ + MnO_3	Pc	156	22.5	28.2	431
$0.925BiFeO_3$–$0.275Ba_{0.85}Ca_{0.15}Ti_{0.90}Zr_{0.10}O_3$ + MnO_2	R	106	24.5	5.93	425

Table 1.3 Energy storage properties of some BF-BT and other lead free piezoceramics (adopted from [90]).

Materials	E (kV/mm)	W_{rec} (J/cm^3)	η (%)	P_{max} (μC/cm^2)	P_r (μC/cm^2)
0.56BFO-0.3BTO-0.14AgNbO$_3$	19.5	2.11	84	–	–
0.65BFO-0.3BTO-0.05Bi(Zn$_{2/3}$Nb$_{1/3}$)O$_3$-0.1wt% MnO$_2$	18	2.06	53	36.7	3.9
BTO-Bi(Mg$_{2/3}$Nb$_{1/3}$)O$_3$	14	1.0509	93	14	0.4
Bi$_{0.5}$Na$_{0.5}$TiO$_3$-BTO-KNbO$_3$	10	0.6497	73	38	5.7
0.61BFO-0.33BTO-0.06Ba(Mg$_{1/3}$Nb$_{2/3}$)O$_3$	12.5	1.17	75	38	7.7
0.62BFO-0.33BTO-0.08Nd(Zn$_{0.5}$Zr$_{0.5}$)O$_3$ (Multilayer)	>70	10.5	87	35	1
0.97(0.65BFO-0.35BTO)-0.03 Nb$_2$O$_5$	9	0.71	–	25.21	5.53
0.61BFO-0.33BTO-0.06La(Mg$_{1/2}$Ti$_{1/2}$)O$_3$	13	~1.66	~82	~37.5	~4.2
0.75(Bi$_{0.85}$Nd$_{0.15}$)FeO$_3$-0.25BTO	18	4.1	~44	40	–
0.6BFO-0.34BTO-0.06Ba(Zn$_{1/3}$Ta$_{2/3}$)O$_3$	16	2.56	>80	–	–
0.6Bi$_{0.98}$La$_{0.02}$FeO$_3$-0.48BTO-0.003MnO$_2$	14	1.22	58	~31	~7

In addition to site engineering, the processing method used to prepare bulk BF-BT-based ceramics also plays a significant role in determining the functional properties [105], [106]. Singh et al. investigated the preparation of BT−BF ceramics using two different sets of initial raw materials: the first set included Bi_2O_3, TiO_2, Fe_2O_3, and $BaCO_3$, while the second set consisted of Bi_2O_3, Fe_2O_3, and $BaTiO_3$. Their findings indicated that using $BaCO_3$ as the initial raw material resulted in superior outcomes compared to $BaTiO_3$. Additionally, they observed the coexistence of tetragonal, rhombohedral, and pseudocubic phases [107]. Quenching has emerged as an innovative approach to enhancing the piezoelectric properties of lead-free BF-based systems. Lee et al. achieved the highest piezoelectric coefficients of 324, 402, and 454 pC/N by water-quenching BF–BT ceramics doped with $Bi(Zn_{1/2}Ti_{1/2})$ and $BiGaO_3$, respectively [31]. The quenching or rapid cooling process has shown significant improvements in the performance of BF–BT-based ceramics when compared to the traditional non-quenching methods such as furnace cooling or slow cooling. This discovery has established quenching as an effective technique for boosting piezoelectricity in BF-based lead-free systems, spurring further research into the effects of quenching variables like temperature and cooling rate. In one such study, Kim et al. in 2016 studied the effect of cooling rate on phase transitions of

BF25BT in which they found better properties in air quenched samples which can be attributed to enhanced rhombohedral distortion and better domain structure as shown in Figure 1.18 [108]. Ji et al., in a separate study, investigated the impact of microwave and conventional sintering methods on the microstructure, electrical, and magnetic properties of a material. The results demonstrated that microwave-sintered samples exhibited a notable reduction in grain size, decreased dielectric loss, and diminished ferroelectric properties [109]. In 2019, Lee et al. reported increment in d_{33} from 240 to 352 pC/N in 0.67BF-0.33BT and 402 to 454 pC/N in 1 mol % $BiGaO_3$ doped 0.67BF-0.33BT by tailoring the cooling and heating process [110].

Lead-free materials are crucial for sustainability but currently have inferior properties compared to lead-based materials. BF-based systems, although relatively new, show promise for high-temperature applications due to their significant piezoelectric properties and high phase transition temperatures. However, they face challenges like high conductivity, primarily due to Bi^{3+} volatilization and Fe ion fluctuation during sintering, leading to high leakage currents. To address these issues, precise compositional design is needed. The pseudo-cubic structure in BF–BT materials enhance piezoelectric properties, as indicated by studies using advanced techniques like in-situ XRD and TEM, which suggest Bi ordering as a key mechanism. Major challenges include processing, crystal structure, and defects, which have been tackled through heat treatment, Bi ion ordering, and doping. Nonetheless, the local structure and mechanisms need further clarification for accurate crystal structure determination, which is essential for new material design methods like structural engineering and MPB control.

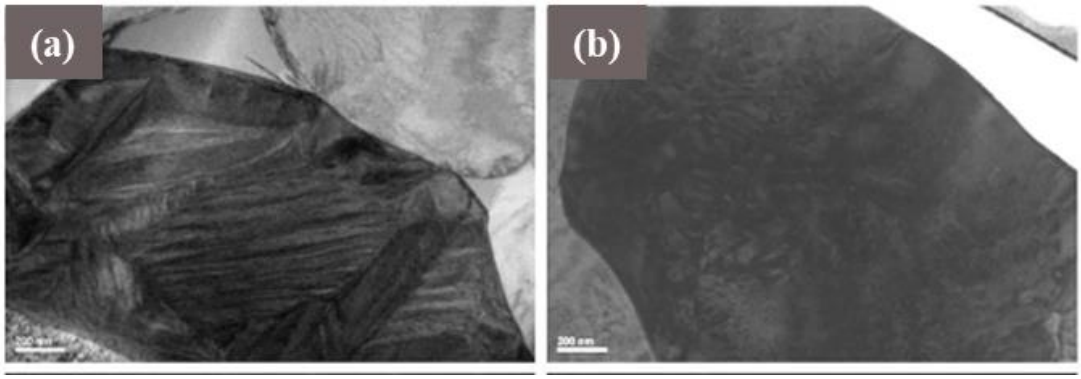

Figure 1.18 Bright field TEM images for BF25BT samples (a) air quenched (AQ) at 800 °C and (b) furnace cooled (FC) (adopted from [108]).

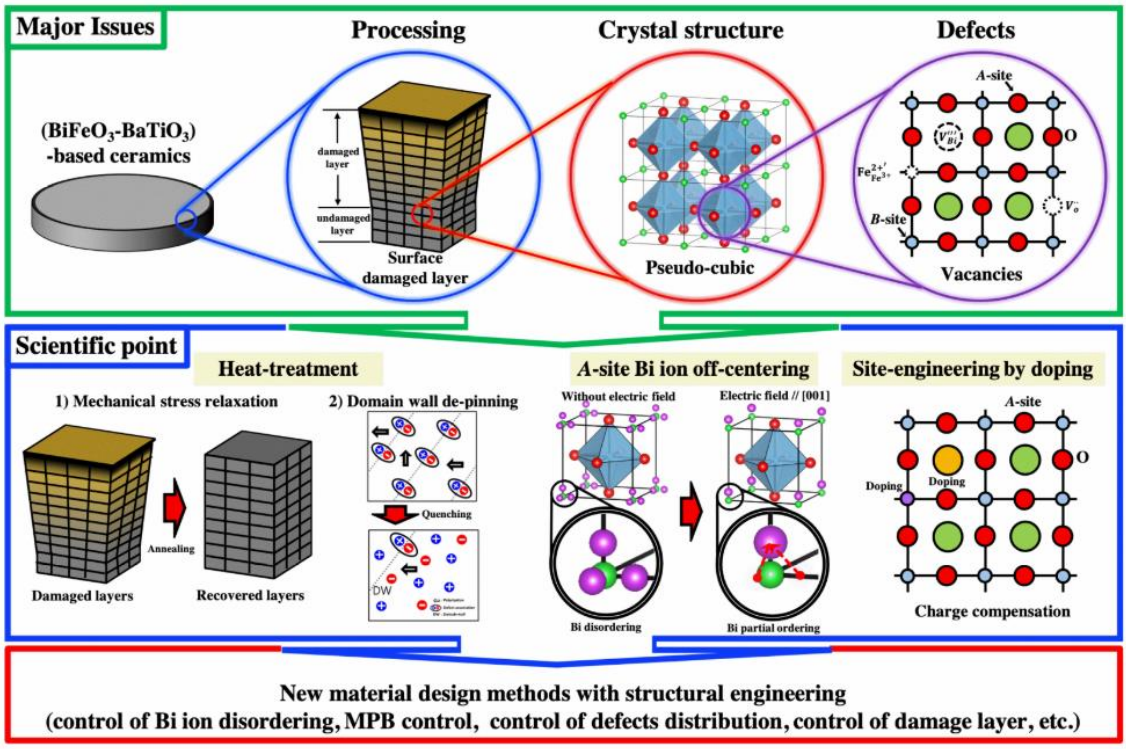

Figure 1.19 Summary of major issues and scientific point in BF based piezoceramics (adopted from [111]).

Recent research has also focused on the magnetic properties, energy harvesting, and dielectric energy storage of BF-based systems, expanding their application potential. This

ongoing research is advancing our understanding of lead-free piezoelectric materials and accelerating the development of next-generation electroactive materials.

1.9.2 $Bi_{0.5}Na_{0.5}TiO_3$ (BNT) Based Ceramics

BNT materials, discovered by Smolenskii et al. in 1960, exhibit a rhombohedral structure. These materials have gained significant attention due to large P_r however they suffer from large E_c and conductivity which hinders poling process resulting in poor piezoelectric properties. A key characteristic of BNT is that chemical modification can create two types of morphotropic phase boundaries (MPB): a R-T phase boundary {MPB(I)} and a ferroelectric-relaxor or polar-nonpolar {MPB(II)} phase boundary. These different phase boundaries induce distinct physical properties in BNT-based materials, with MPB(I) leading to high d_{33} and MPB(II) resulting in large strain [112]. In 2007, Zang and colleagues reported a substantial strain value (S=0.45%) in BNT-BT-KNN ternary ceramics with MPB(II), comparable to strains in lead-based materials due to an antiferroelectric to ferroelectric phase transition [113]. For instance, the creation of an R-T phase boundary in ceramics (1−x)BNT-xBT (x=0.06) was found to boost piezoelectricity (d_{33}=122-174 pC/N) as listed in Table 1.4 [112]. Perhaps BNT-based ceramics can achieve a high d_{33} of approximately 231 pC/N due ion substitution see Table 1.5. By 2016, Tan and co-authors achieved a superior strain value of 0.7% and d_{33}^* of 1400 pm/V in Sr and Nb co-modified BNT-based ceramics [114]. Large strain values are essential for actuator applications, but BNT-based ceramics face practical challenges due to low depolarization temperatures and significant hysteresis, which limit their operational temperature range. Even with composition modifications to widen the temperature usage range, the piezoelectric coefficient remains insufficient for practical applications.

Table 1.4 Electrical characteristics of BNT-BT ceramics (adopted from [4]).

Material system	Phase structure	d_{33} (pC/N)	k_p	T_m (°C)	T_d (°C)
$0.94Bi_{1/2}Na_{1/2}TiO_3$-$0.06BaTiO_3$	R-T	125	0.2	288	
$0.94Bi_{1/2}Na_{1/2}TiO_3$-$0.06BaTiO_3$	R-T	122	0.29	225	100
$0.94Bi_{1/2}Na_{1/2}TiO_3$-$0.06BaTiO_3$	R-T	155	0.367		105
$0.94Bi_{1/2}Na_{1/2}TiO_3$-$0.06BaTiO_3$	R-T	148	–		
$0.93Bi_{1/2}Na_{1/2}TiO_3$-$0.07BaTiO_3$	R-T	134	–	305	165
$0.925Bi_{1/2}Na_{1/2}TiO_3$-$0.075BaTiO_3$	R-T	186	–		
$0.935Bi_{1/2}Na_{1/2}TiO_3$-$0.065BaTiO_3$	R-T	150	0.51 (k_t)		
$0.94Bi_{1/2}Na_{1/2}TiO_3$-$0.06BaTiO_3$	R-T	174	0.28		

Table 1.5 Electrical characteristics of BNKT ceramics after ion substitution (adopted from [4]).

Material system	Phase structure	d_{33} (pC/N)	Strain (%)	d_{33}^* (pm/V)
$Bi_{1/2}(Na_{0.7}K_{0.2}Li_{0.1})_{1/2}TiO_3$		231		
$Bi_{1/2}(Na_{0.78}K_{0.2}Ag_{0.02})_{1/2}TiO_3$	R	180		
$Bi_{1/2}(Na_{0.78}K_{0.22})_{1/2}(Ti_{0.97}Hf_{0.03})O_3$			0.38	475
$Bi_{1/2}(Na_{0.78}K_{0.22})_{1/2}(Ti_{0.97}Zr_{0.03})O_3$		31	0.43	614
$Bi_{1/2}(Na_{0.82}K_{0.18})_{1/2}(Ti_{0.97}Nb_{0.03})O_3$	RT-Pc		0.47	641
$Bi_{1/2}(Na_{0.82}K_{0.18})_{1/2}(Ti_{0.98}Ta_{0.02})O_3$	RT-Pc		0.34	566
$Bi_{1/2}(Na_{0.78}K_{0.22})_{1/2}(Ti_{0.95}Sn_{0.05})O_3$	T-Pc		0.35	585
$[Bi_{1/2}(Na_{0.82}K_{0.18})_{1/2}]_{0.97}Li_{0.03}TiO_3$		110		250
$[Bi_{1/2}(Na_{0.82}K_{0.18})_{1/2}]_{1-x}La_xTiO_3$		172 (x = 0.02)		650 (x = 0.03)
$(Bi_{0.5}Na_{0.78}K_{0.18}Li_{0.04})_{0.5}(Ti_{0.95}Sn_{0.05})O_3$	T-Pc		0.39	646
$(Bi_{0.5}Na_{0.385}K_{0.09}Li_{0.025})(Ti_{0.975}Ta_{0.025})O_3$	RT-Pc		0.436	727
$\{[Bi_{0.5}(Na_{0.84}K_{0.16})_{0.5}]_{0.96}Sr_{0.04}\}Ti_{0.975}Nb_{0.025}O_3$	*R*3c-*P*4bm		0.70	1400

1.9.3 $Bi_4Ti_3O_{12}$ (BIT) Based Piezoceramics

Bismuth layered structure ferroelectrics (BLSFs) have been extensively researched due to their unique structural characteristics, high T_C (usually above 500 °C), and promising ferroelectric properties. BLSFs are characterized by their layered perovskite structures, where bismuth oxide layers interleave with ferroelectric perovskite blocks. This structure confers high thermal stability and robust ferroelectric properties. The general formula for these materials is $(Bi_2O_2)^{2+}(A_{n-1}B_nO_{3n+1})^{2-}$, where 'A' and 'B' are cations in the perovskite block, and 'n' denotes the number of BO_6 octahedra [115]. Aurivillius phases are a type of layered oxide material consisting of alternating $[Bi_2O_2]^{2+}$ layers and perovskite-type layers, forming a sandwich-like structure[116]. These materials have garnered significant attention due to their potential applications in nonvolatile memories, photocatalysis and high-temperature piezoelectric devices [117], [118], [119], [120], [121], [122], [123], [124]. Their distinctive ferroelectric and piezoelectric properties arise from the rotation

of BO_6 octahedra, which lowers the symmetry from tetragonal to orthorhombic, and allows the A and B-site cations in the perovskite layers to be displaced relative to the oxygen anion array. This structural change is key to their unique properties. Despite the wide range of materials within the Aurivillius family, none have yet perfectly met the requirements for multifunctional commercial applications. As a result, there is continuous interest and ongoing research aimed at improving the electrical properties of these layered ferroelectrics to make them suitable for practical use [125]. However, their practical application is hindered by weak piezoelectric performance due to the interference of the two-dimensional layer structure and the weak coupling of polar octahedra [3]. Additionally, these materials have certain drawbacks, such as a high coercive field and suboptimal ferroelectric and piezoelectric properties. Among BLSFs, BIT is one of the earliest investigated and stands out as a material of significant interest, especially for high-temperature applications and lead-free piezoceramics. Its functional properties can be significantly enhanced through chemical modification. In the past, techniques such as ion doping, and various synthesis methods have often been utilized to boost the electrical performance of BIT-based ceramics. Due to the absence of phase boundaries, much of the research has concentrated on modifying the composition to enhance their ferroelectric and piezoelectric characteristics.

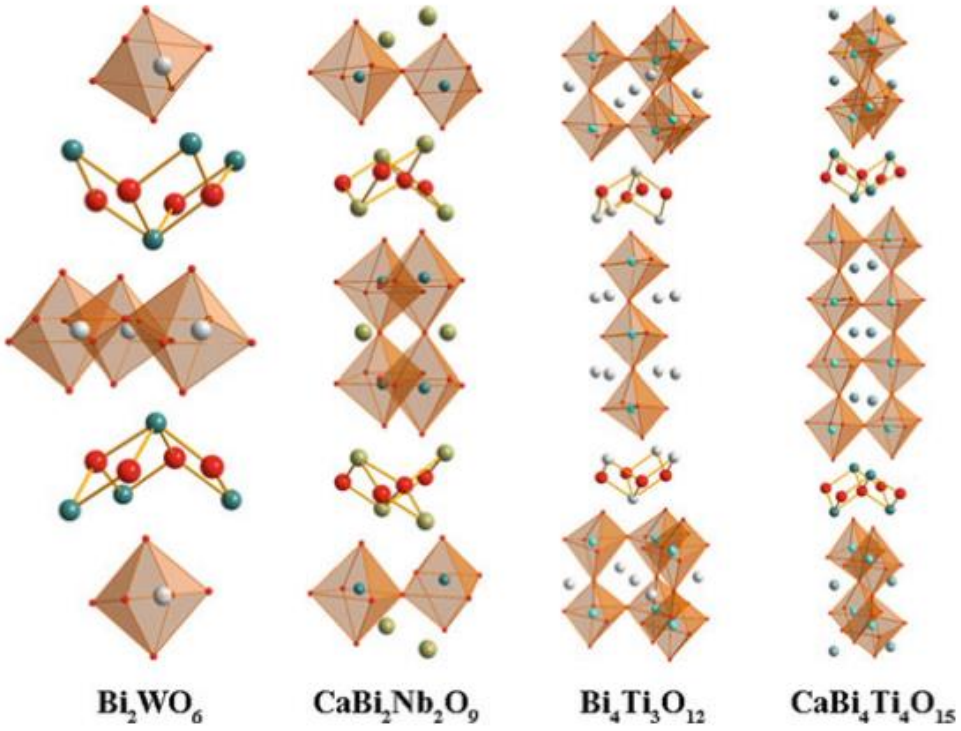

Figure 1.20 Ball stick model of different BLSFS (adopted from [126]).

Typically, the Bi atom at the A-site in the perovskite layer can be substituted by ions with ionic radii ranging from 1.1 to 1.3 Å, while ions with radii between 0.58 and 0.65 Å can replace the Ti^{4+} at the B-site. For the structural stability of Aurivillius compounds, the tolerance factor and inter-strain (or mismatch) are crucial. Ion substitution influences both these factors. Large cations that can occupy the A-site include Na^{+}, K^{+}, Ca^{2+}, Sr^{2+}, Ba^{2+}, Pb^{2+}, Y^{3+}, and various lanthanides such as La, Nd, Sm, Gd, Ce, Tb, Dy, Er, Eu, Yb, etc. [123], [124], [127], [128], [129], [130], [131], [132], [133], [134], [135], [136], [137], [138], [139], [140], [141], [142], [143], [144], [145], [146]. The B-site can incorporate aliovalent elements like Fe^{3+}, Cr^{3+}, W^{6+}, Nb^{5+}, Ta^{5+}, V^{5+}, Cu^{2+}, Mo^{6+}, and Mg^{2+} [117], [123], [124], [127], [131], [132], [133], [134], [135], [138], [141], [146], [147], [148], [149], [150], [151], [152], [153], [154], [155], [156], [157], [158], [159], [160], [161],

[162]. BIT exhibits anisotropic properties due to its crystal structure. It has platelet like microstructure that primarily grows in ab plane. It exhibits significantly higher electrical conductivity and spontaneous polarization values in the ab plane compared to the c-axis, with the difference being about an order of magnitude which hinders the poling process and overall functional properties. At high temperatures, intrinsic oxygen vacancies are considered the main defect, while at lower temperatures, electron holes become the predominant carriers, negatively impacting electrical properties [163]. One of the primary challenges for BIT-based materials is achieving high electrical resistivity, which is crucial for efficient poling of the ceramics and for their effective use in high-temperature devices. The site engineering method effectively improves electrical behavior, although it tends to lower the T_C. For instance, in a study conducted by Shulman et al. the conductivity of BIT was reduced by the order of 3 magnitude by using Nb donor dopant which led to improved d_{33}~20pC/N [146]. In other study, La-doping at the A-site in BIT films has been reported to improve remnant polarization to P_r=12 μC/cm^2 and enhance fatigue properties [164]. B-site substitutions with donor dopants such as V^{5+}, Nb^{5+}, Ta^{5+}, and W^{6+} have been found to increase electrical resistivity by 1–3 orders of magnitude compared to undoped BIT, while also boosting the piezoelectric coefficient d_{33} to 16–32 pC/N [150], [152], [163], [165]. This improvement is largely attributed to donor doping at the B-site, which reduces intrinsic oxygen vacancies or electron hole concentration through charge compensation effects and causes a greater deviation in the nearly rigid framework along the a-direction of the [B_mO_{3m+1}] segment of the perovskite layers. Recent studies have shown that codoping Aurivillius ceramics enhances their pyroelectric and piezoelectric coefficients, while also reducing relative permittivity and dielectric loss [139], [141], [150], [151], [157], [159], [161], [166], [167], [168], [169], [170], [171], [172], [173]. In 2022, Xie et al. reported a notable d_{33} of 40.2 pC/N and a high T_C of 657 °C**,** the highest reported till

date in $Bi_{3.97}Ce_{0.03}Ti_{2.98}(WNb)_{0.01}O_{12}$ ceramics [174]**.** Analyses of their electrical properties and microstructure attribute this high piezoelectricity to the preferential orientation of ferroelectric domains, irreversible ferroelectric domain reorientation, and a high density of domain walls. These improvements make the materials highly suitable for pyroelectric and piezoelectric device applications. This demonstrates that strategic doping with multiple dopants is an effective method for enhancing the electrical properties of Aurivillius compounds. Studies have demonstrated that sintering temperature plays a crucial role in affecting these properties [175]. For instance, Xu et al. discovered that on increasing the sintering temperature from 1060 ℃ to 1140 ℃ increased the grain size and enhanced the d_{33} values in Ce/W/Nb codoped BIT from 28.40 to 34.30 pC/N, as shown in Figure 1.21. By applying new preparation techniques for chemical modification, high piezoelectric constants can be achieved, along with improved ferroelectric properties due to reduced coercive fields [171]. Additionally, the hot-forging technique enables a large piezoelectric constant of approximately 49.5 pC/N in $Bi_{3.7}Sr_{0.3}Ti_{2.7}Ta_{0.3}O_{12}$ ceramics [176]. In 2013, Chen et al. prepared ceramics with grain sizes from 4.2 μm to 0.28 μm using normal sintering, two-step sintering, and hot-pressing sintering methods. Internal stress and poling electric field strength both affect the ferroelectric domain switching in BIT ceramics. An optimal d_{33} of 6.8 pC/N was achieved with a grain size of 0.57 μm. However, internal stresses, which drive thermal depolarization, increased as grain size decreased, resulting in reduced thermal stability [177]. In 2023, Liang et al. found that by using direct reaction sintering method in Mn/Ta codoped BIT more uniform grain distribution and higher density can be obtained which resulted in improved resistivity of 7.19×10^5 Ω cm at 500 °C, high residual polarization (8.1 μC/cm²), and an excellent piezoelectric coefficient (31 pC/N) [150]. Hence, chemical modifications (or in

conjunction with new preparation techniques) can significantly enhance the ferro/piezoelectric properties of $Bi_4Ti_3O_{12}$ ceramics.

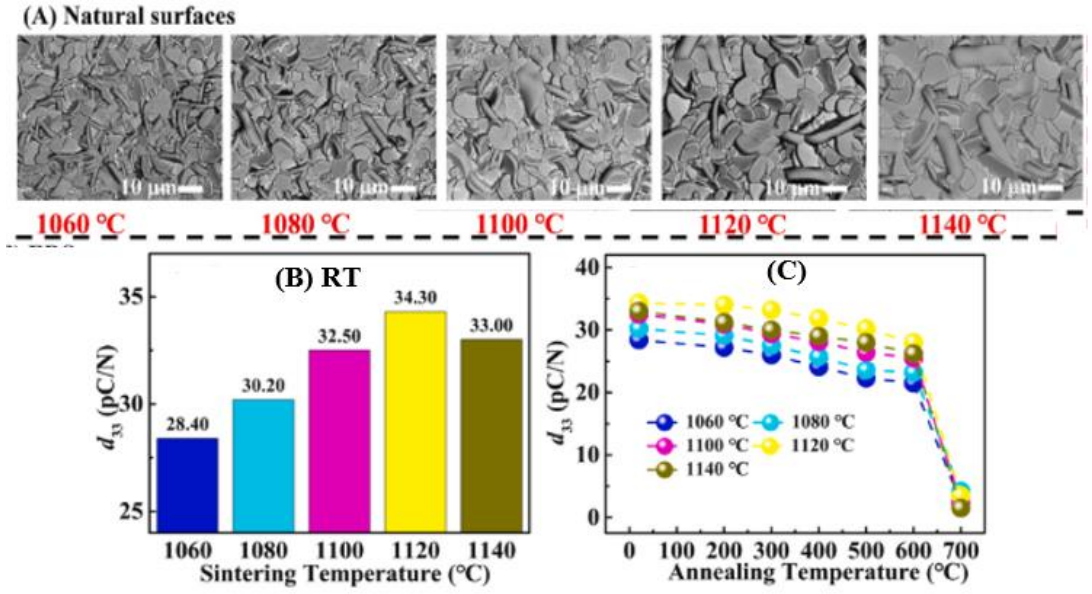

Figure 1.21 (A) SEM micrographs at different sintering temperature, (B) variation of d_{33} as a function of sintering temperature measured at RT, and (C) d_{33} as a function of annealing temperature (adopted from [145]).

By reviewing the progression of BLSFs, it is evident that the piezoelectric charge constant (d_{33}) and Curie temperature (T_C) of BLSF ceramics are largely determined by their chemical compositions. Figure 1.22 displays the relationship between d_{33} and T_C for BLSF ceramics made through the conventional sintering method. There is significant variation in the d_{33} and T_C values of BLSF ceramics. Generally, improving piezoelectric properties tends to lower the T_C. For applications with operating temperatures above 400 °C, only a limited number of materials are suitable for practical piezoelectric devices. BLSFs strike a good balance between d_{33} and T_C, making them ideal for high-temperature piezoelectric applications. Additionally, chemical modifications and advanced preparation techniques are effective in enhancing the electrical properties of BLSF

materials. Therefore, selecting material systems with the appropriate d_{33} and T_C can be customized to meet specific application requirements.

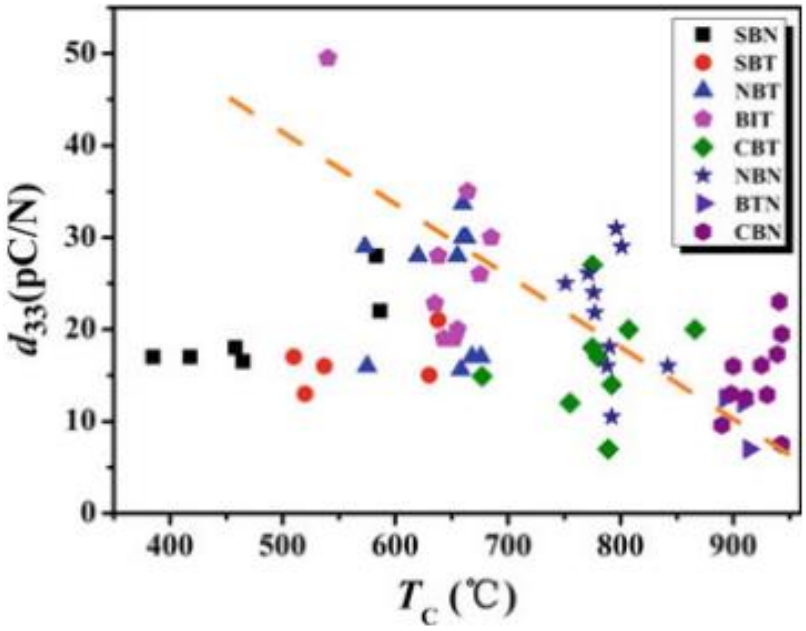

Figure 1.22 d_{33} vs Tc variation of different BSLFs (adopted from [126]).

1.10 Objective of Present Work

The primary objective of this thesis is to develop Bi-based lead-free piezoelectric perovskite ceramics for high-temperature energy harvesting applications. This research aims to develop novel lead-free compositions with enhanced functional properties including good thermal stability and energy harvesting efficiency. By systematically exploring the synthesis, characterization, and performance optimization of Bi-based normal and layered perovskite ceramics, this thesis seeks to contribute significantly to the field of sustainable and high-performance multifunctional piezoelectric materials, providing viable alternatives to lead-based systems and supporting the development of environmentally friendly technologies.

Specifically, the objectives are as follows:

1. Comparative Study of Sintering Methods:
    - Conduct a detailed comparative study between closed sintering and air quenching methods in Sc, Ga modified BF-BT based relaxor piezoceramics to determine the preferable method for the chosen composition.
    - Evaluate the influence of processing methods their effects on the structural and functional properties of the ceramics, including phase structure, microstructure, dielectric, ferroelectric, and piezoelectric properties.
2. Development of Novel Bi-based Lead-free Compositions
    - To develop a novel Bi-based lead-free compositions using site engineering suitable for high temperature application and to examine the structural, morphological, absorption, optical, dielectric and ferroelectric properties and piezoelectric properties of the various compositions.
3. Improve Energy Harvesting Efficiency:
    - Develop and optimize fabrication techniques to increase the energy harvesting efficiency of these ceramics, making them viable alternatives to lead-based systems.
4. Site Engineering for Property Enhancement:
    - Explore the effects of co-doping the A-site and/or B-site in BIT ceramics to significantly enhance their electrical resistivity and ferroelectric/piezoelectric properties. This involves identifying suitable dopants that can reduce

conductivity and achieve a balance between good polarizability and a high ferroelectric phase transition temperature.

5. Effect of Sintering Temperature
    - Investigating the effects of varying sintering temperature on the crystal structure, morphology, optical, dielectric, ferroelectric and piezoelectric properties.

By addressing these objectives, this thesis aims to elucidate the mechanisms that enhance the high-temperature capabilities of Bi-based ceramics and develop guidelines for their application in energy harvesting systems.